

## IMPLICIT A POSTERIORI ERROR ESTIMATES FOR THE MAXWELL EQUATIONS

FERENC IZSÁK, DAVIT HARUTYUNYAN, AND JAAP J.W. VAN DER VEGT

**ABSTRACT.** An implicit a posteriori error estimation technique is presented and analyzed for the numerical solution of the time-harmonic Maxwell equations using Nédélec edge elements. For this purpose we define a weak formulation for the error on each element and provide an efficient and accurate numerical solution technique to solve the error equations locally. We investigate the well-posedness of the error equations and also consider the related eigenvalue problem for cubic elements. Numerical results for both smooth and non-smooth problems, including a problem with reentrant corners, show that an accurate prediction is obtained for the local error, and in particular the error distribution, which provides essential information to control an adaptation process. The error estimation technique is also compared with existing methods and provides significantly sharper estimates for a number of reported test cases.

### 1. INTRODUCTION

The solution of the Maxwell equations frequently contains structures with limited regularity, such as singularities near corners and non-convex edges. These structures can be efficiently captured using  $hp$ -adaptive techniques, in which the mesh is locally refined and coarsened ( $h$ -adaptation) or the polynomial order in individual elements is adjusted ( $p$ -adaptation). Examples of  $hp$ -adaptive techniques applied to the Maxwell equations can be found in e.g. [12, 16, 24, 25, 26, 29]. The  $hp$ -adaptation technique is a promising approach to obtain efficient numerical algorithms to solve the Maxwell equations, but requires a reasonably accurate estimate of the local error in the numerical solution in order to control the adaptation process. In simple cases one can predict the regions which need to be adapted, but a more general approach requires the use of a posteriori error estimates in which the local error is predicted based on the numerical solution. General techniques for a posteriori error estimation are discussed in e.g. [1], [3], [4], [17], [18], [28], but providing accurate a posteriori error estimates for the Maxwell equations still poses many problems.

In the a posteriori error analysis of the Maxwell equations one encounters two basic problems: the bilinear form of the Maxwell equations is in general not coercive, and the analytic solution is not necessarily smooth. Moreover, in real-life situations

---

Received by the editor February 1, 2006 and, in revised form, February 24, 2007.

2000 *Mathematics Subject Classification.* Primary 65N15, 65N30, 65R20.

*Key words and phrases.* Maxwell equations, a posteriori error estimates, implicit estimates, Nédélec edge finite elements.

This research was supported by the Dutch government through the national program BSIK: knowledge and research capacity, in the ICT project BRICKS (<http://www.bsik-bricks.nl>), theme MSV1.

computations often have to be done in three-dimensional domains of complex geometry (e.g. with reentrant corners) and consisting of different materials (so that the coefficients of the equations are discontinuous). To avoid these difficulties, several studies [6], [7], [23] only investigate a problem defined by a coercive bilinear form. Others, e.g. [21], assume some regularity in the solution of the dual problem.

There are several techniques to obtain a posteriori error bounds for the Maxwell equations. Explicit methods, see e.g. [6], [21], give an error estimate based on the available numerical solution and are relatively easy to implement. The error bounds in explicit methods contain in general unknown coefficients, which also depend on the wave number in the equations, and frequently result in unsharp estimates. Another approach is provided by using a hierarchical basis; see e.g. [1], [5]. This approach has been applied in [7] to the (curl) elliptic Maxwell equations. The analysis of this method is based on some assumptions, such as the saturation assumption ([1, Section 5.2]), and the replacement of the bilinear form by an equivalent (localized) bilinear form which ignores coupling terms to obtain a small linear system for the error equations. The validity and effect of these assumptions on the accuracy requires, however, careful attention. Implicit error estimators for the Maxwell equations have been developed in [26], based on the approach in [14], and successfully applied to an *hp* adaptive finite element algorithm for the Maxwell equations in 3D. Lacking a complete analysis, the authors applied an equilibration technique to ensure well-posedness which results in a rather complicated computational procedure.

In this paper we further investigate the use of implicit error estimators. We follow an approach originally developed for elliptic partial differential equations (see e.g. [1]) which when properly formulated, is also applicable to obtain local error estimates for the Maxwell equations. For this purpose, we first define a weak formulation for the error in each element, which is solved with a finite element method. This is the main difference with explicit a posteriori error estimates which only use the data provided by the numerical solution. We consider the time-harmonic Maxwell equations with perfectly conducting boundaries discretized with Nédélec edge elements, but many ideas can be applied in a more general setting. The main benefit of implicit error estimates is that we do not encounter unknown or very large constants in the a posteriori error estimates. The success of this approach, however, strongly depends on the definition of the boundary conditions for the local error equations and the choice of a proper basis for the numerical solution of the local problems. The latter is achieved by using higher order face and element bubble functions.

The second topic we address is the theoretical properties of the implicit a posteriori error estimation technique. First, we investigate the well-posedness of the weak formulation for the local error, in particular in relation to the boundary conditions used in the local error equations. Also, the eigenvalue problem related to the local error equations is investigated in detail. Following the lines in [1] we introduce an error indicator and point out that this provides a lower bound for the exact error and an upper bound for our implicit estimate (up to a constant factor in both cases). These results give the implicit a posteriori error estimation technique a sound theoretical basis and make it possible to avoid some of the involved techniques used in [26], [29].

Instead of giving sharp error estimates we check the preciseness of our method using numerical experiments. We pay special attention to cases where the analytic solution is non-smooth and also investigate the problem in computational domains with reentrant corners. Both the local and global error are estimated in the  $H(\text{curl})$  norm and compared with the exact error. We also consider the error distribution, since this is essential information to decide in which areas the mesh has to be adapted. Despite of the expected difficulties we obtain rather precise estimates in each case.

The outline of the paper is as follows. In Section 2 we start with the mathematical formulation and define the finite element discretization. The implicit error estimation technique is formulated and analyzed in Section 3. Next, we discuss lower and upper bounds on the error indicator in Section 4. The implicit a posteriori error estimation technique is tested numerically on a number of problems of increasing difficulty in Section 5. Finally, Section 6 contains conclusions and suggestions for future work.

In this paper we frequently use notations and techniques discussed in the monograph [21]. For a short, self-contained introduction to finite element methods for the Maxwell equations we refer to [15].

## 2. MATHEMATICAL FORMALIZATION

Consider the time harmonic Maxwell equations for the electric field  $\mathbf{E} : \Omega \rightarrow \mathbb{R}^3$  with perfectly conducting boundary conditions, which are defined as

$$(1) \quad \begin{aligned} \text{curl curl } \mathbf{E} - k^2 \mathbf{E} &= \mathbf{J}_k \quad \text{in } \Omega, \\ \mathbf{E} \times \boldsymbol{\nu} &= 0 \quad \text{on } \partial\Omega, \end{aligned}$$

where  $\Omega \subset \mathbb{R}^3$  is a Lipschitz domain with outward normal vector  $\boldsymbol{\nu}$  and  $\mathbf{J}_k \in [L_2(\Omega)]^3$  is a given source term which is related to the wave number  $k$ . Here  $k = \frac{\omega}{c}$  with the frequency  $\omega$  and the speed of light  $c$ . Here  $\mathbf{E} \times \boldsymbol{\nu}$  is defined in a trace sense [10], [21] discussed later.

In the subsequent derivations we will need the following spaces and operators.

The Hilbert space corresponding to the Maxwell equation is

$$H(\text{curl}, \Omega) = \{\mathbf{u} \in [L_2(\Omega)]^3 : \text{curl } \mathbf{u} \in [L_2(\Omega)]^3\},$$

equipped with the curl norm

$$(2) \quad \|\mathbf{u}\|_{\text{curl}, \Omega} = (\|\mathbf{u}\|_{[L_2(\Omega)]^3}^2 + \|\text{curl } \mathbf{u}\|_{[L_2(\Omega)]^3}^2)^{1/2}.$$

The differential operators  $\text{div}$  and  $\text{curl}$  are understood in a distributional sense. While analyzing (1) a subspace of  $H(\text{curl}, \Omega)$  is commonly used, namely

$$H_0(\text{curl}, \Omega) = \{\mathbf{u} \in H(\text{curl}, \Omega) : \boldsymbol{\nu} \times \mathbf{u}|_{\partial\Omega} = 0\}.$$

The above definition of  $H_0(\text{curl}, \Omega)$  makes sense only if  $\mathbf{u}|_{\partial\Omega}$  is well defined and a duality between this trace and the outward normal can be defined. To be more precise we first define for a smooth function  $\mathbf{v} \in C^\infty(\Omega)$  the operators  $\gamma_\tau$  and  $\pi_\tau$  with

$$(3) \quad \gamma_\tau \mathbf{v} = \boldsymbol{\nu} \times \mathbf{v}|_{\partial\Omega} \text{ and } \pi_\tau \mathbf{v} = (\boldsymbol{\nu} \times \mathbf{v}|_{\partial\Omega}) \times \boldsymbol{\nu}.$$

One can prove that  $\gamma_\tau$  can be extended to a continuous operator mapping  $H(\text{curl}, \Omega)$  into  $[H^{-1/2}(\partial\Omega)]^3$ . The trace operator  $\pi_\tau$  can also be extended to  $H(\text{curl}, \Omega)$ , however, a natural norm on the range is more involved. For the details we refer to

[21], or for a more extensive analysis to [11]. The above definitions and notations will also be used for a subdomain  $K \subset \Omega$ .

The scalar product in  $[L_2(\Omega)]^3$  and  $[L_2(K)]^3$  are denoted with  $(\cdot, \cdot)$  and  $(\cdot, \cdot)_K$ , respectively. Similarly,  $(\cdot, \cdot)_{\partial\Omega}$  and  $(\cdot, \cdot)_{\partial K}$  denote the duality pairing between the two types of traces on  $\partial\Omega$  and  $\partial K$ , respectively.

We also recall an appropriate Green’s formula: for any  $\mathbf{u}, \mathbf{v} \in H(\text{curl}, \Omega)$  we have the identity

$$(4) \quad (\text{curl } \mathbf{u}, \mathbf{v}) - (\mathbf{u}, \text{curl } \mathbf{v}) = (\gamma_\tau \mathbf{u}, \pi_\tau \mathbf{v})_{\partial\Omega}, \quad \forall \mathbf{u}, \mathbf{v} \in H(\text{curl}, \Omega),$$

and a corresponding formula holds on  $K$ .

Turning to the variational formulation of (1) we introduce the bilinear form

$$B : H(\text{curl}, \Omega) \times H(\text{curl}, \Omega) \rightarrow \mathbb{R}$$

with

$$B(\mathbf{u}, \mathbf{v}) = (\text{curl } \mathbf{u}, \text{curl } \mathbf{v}) - k^2(\mathbf{u}, \mathbf{v}),$$

and  $B_K$  will denote the corresponding bilinear form on  $H(\text{curl}, K) \times H(\text{curl}, K)$ .

Using the above notations the weak formulation of the problem (1) is to find  $\mathbf{E} \in H_0(\text{curl}, \Omega)$  such that

$$(5) \quad (\text{curl } \mathbf{E}, \text{curl } \mathbf{v}) - k^2(\mathbf{E}, \mathbf{v}) = (\mathbf{J}_k, \mathbf{v}) \quad \forall \mathbf{v} \in H_0(\text{curl}, \Omega).$$

**2.1. Finite elements in  $H(\text{curl})$ : Edge elements.** For the numerical solution of (5) we use the  $H(\text{curl})$  conforming edge finite element method initiated by Nédélec [22].

The finite element  $(\hat{K}, \hat{P}, \hat{\mathcal{A}})$  [8] is defined on the unit cube  $\hat{K}$ , and an isoparametric mapping ([8], Section 4.7)  $D_K : \hat{K} \rightarrow K$  is used to define it on a hexahedron  $K$ . In general,  $D_K$  could be non-linear, but we restrict the analysis to affine maps.

In the numerical experiments we use the lowest order elements

$$(6) \quad \hat{P} = \{\mathbf{u} = [u_1, u_2, u_3]^t : u_1 \in Q_{0,1,1}; u_2 \in Q_{1,0,1}; u_3 \in Q_{1,1,0}\},$$

with  $Q_{k,l,m}$  the vector space of  $k, l$  and  $m$  order polynomials with respect to their first, second and third variables, respectively.

It is well known that the covariant transformation preserves line integrals under a change of coordinates [21, 27], so that the basis functions for a given hexahedron  $K$  can be defined as

$$(7) \quad \mathbf{w}_{j,K}(x, y, z) = ((dD_K^{-1})^T \mathbf{W}_j^0) \circ D_K^{-1}(x, y, z),$$

where  $dD_K$  is the Jacobian of the transformation  $D_K$ , and  $\{\mathbf{W}_j^0\}_{j=1}^{12}$  is a basis in (6).

Using the transformation in (7) one easily computes the curl of the basis functions (see [21], (3.76) and the corresponding statements: Lemma 3.57, Corollary 3.58). A similar transformation for divergence conforming finite elements ([21, (3.77)]) is well known and called the Piola transformation ([20, p. 112]).

Next, we introduce a hexahedral tessellation  $\mathcal{T}_h$  of  $\Omega$ . The space  $W_h$  of Nédélec’s edge elements is then defined by

$$W_h = \{\mathbf{u}_h \in H(\text{curl}, \Omega) : \mathbf{u}_h|_K \in \text{span}(w_{j,K}), \forall K \in \mathcal{T}_h\},$$

where  $\text{span}(w_{j,K})$  denotes the linear hull of  $w_{1,K}, w_{2,K}, \dots, w_{12,K}$ , and with this the discretized version of (5) reads:

Find  $\mathbf{E}_h \in W_h$ , such that for all  $\mathbf{W} \in W_h$  the following relation is satisfied:

$$(8) \quad (\text{curl } \mathbf{E}_h, \text{curl } \mathbf{W}) - k^2(\mathbf{E}_h, \mathbf{W}) = (\mathbf{J}_k, \mathbf{W}).$$

### 3. IMPLICIT ERROR ESTIMATION

Providing reliable explicit bounds for the computational error in the case of the Maxwell equations is still an unsolved problem due to many difficulties as mentioned in the Introduction. The idea of implicit a posteriori error estimation can help to overcome these problems. In this procedure we are not interested in explicit error bounds (depending on the data from some existing numerical approximation), rather, we formulate a local problem for the error using the available information. This local problem has to be equipped with some meaningful boundary condition and we have to ensure that it is well posed.

**3.1. Formulation of the local problem.** Assume that  $\mathbf{E}_h$  is a computed numerical solution. Our aim is to estimate the computational error  $e_h = (\mathbf{E} - \mathbf{E}_h)|_K$  on a subdomain  $K$  consisting of a set of elements  $K \in \mathcal{T}_h$ , with  $\mathcal{T}_h$  being the finite element tessellation. For this we state a variational problem for  $e_h$  on the subdomain  $K$  as follows:

$$(9) \quad \begin{aligned} B_K(e_h, \mathbf{v}) &= (\text{curl } e_h, \text{curl } \mathbf{v})_K - k^2(e_h, \mathbf{v})_K \\ &= (\text{curl } (\mathbf{E} - \mathbf{E}_h), \text{curl } \mathbf{v})_K - k^2(\mathbf{E} - \mathbf{E}_h, \mathbf{v})_K \\ &= (\text{curl } \mathbf{E}, \text{curl } \mathbf{v})_K - k^2(\mathbf{E}, \mathbf{v})_K - ((\text{curl } \mathbf{E}_h, \text{curl } \mathbf{v})_K - k^2(\mathbf{E}_h, \mathbf{v})_K) \\ &= (\text{curl curl } \mathbf{E}, \mathbf{v})_K - (\gamma_\tau \text{curl } \mathbf{E}, \pi_\tau \mathbf{v})_{\partial K} - k^2(\mathbf{E}, \mathbf{v})_K - B_K(\mathbf{E}_h, \mathbf{v})_K \\ &= (\mathbf{J}_k, \mathbf{v})_K - (\gamma_\tau \text{curl } \mathbf{E}, \pi_\tau \mathbf{v})_{\partial K} - B_K(\mathbf{E}_h, \mathbf{v}), \quad \forall \mathbf{v} \in H(\text{curl}, K). \end{aligned}$$

In order to get a well defined right hand side we should use an approximation

$$(10) \quad \gamma_\tau \text{curl } \mathbf{E} \approx \widehat{\gamma_\tau \text{curl } \mathbf{E}}$$

on the interelement faces. The quantity  $\widehat{\gamma_\tau \text{curl } \mathbf{E}}$  will be called the *natural* boundary data from now on. In the literature, the homogeneous natural boundary condition is called the magnetic symmetry wall condition [15]. Introducing this approximation into (9) we arrive at the variational problem for the implicit error estimate: Find  $\hat{e}_h \in H(\text{curl}, K)$  such that

$$(11) \quad B_K(\hat{e}_h, \mathbf{v}) = (\mathbf{J}_k, \mathbf{v})_K - (\widehat{\gamma_\tau \text{curl } \mathbf{E}}, \pi_\tau \mathbf{v})_{\partial K} - B_K(\mathbf{E}_h, \mathbf{v}), \quad \forall \mathbf{v} \in H(\text{curl}, K).$$

**3.2. Numerical solution of the local problem.** We will now give a discretized form of the local problem (11) which requires a concrete choice for the approximation (10) of the natural boundary condition and a finite element basis on the subdomain  $K$ .

**3.2.1. Approximation of the natural boundary condition.** We first specify the approximation in (10). For the definition of the boundary condition for the local error equation (10) we introduce  $l_j$  as the common face of the two neighboring elements  $K$  and  $K_j$  and  $\boldsymbol{\nu}_j$  as the outward normal on  $l_j$  with respect to  $K$ . We approximate  $\widehat{\gamma_\tau \text{curl } \mathbf{E}}$  on  $l_j$  with the average of the tangential traces of the numerical approximation  $\mathbf{E}_h$  on its two sides  $K$  and  $K_j$ . That is, we shall use the approximation

$$(12) \quad \widehat{\gamma_\tau \text{curl } \mathbf{E}}|_{l_j} = \boldsymbol{\nu}_j \times \text{curl } \mathbf{E}|_{l_j} \approx \frac{1}{2}(\boldsymbol{\nu}_j \times [\text{curl } \mathbf{E}_h|_K + \text{curl } \mathbf{E}_h|_{K_j}])$$

which can be straightforwardly implemented.

3.2.2. *Choice of the local basis.* The local error equation (cf. (11)) is solved numerically in a finite-dimensional space which we denote with  $V_h$ . As discussed in [1] (see Section 3.4.2 in [1] for several examples), the space  $V_h$  has to be selected carefully.

It is known that the finite element solution  $\mathbf{E}_h$  is a quasioptimal approximation of  $\mathbf{E}$  within the finite element space  $W_h$ . Therefore, it does not make sense to use this space to solve the error equation; we should rather estimate the components of  $\hat{\mathbf{e}}_h$  which are not present in  $W_h$ .

On the other hand, Nédélec type edge elements are related to the electric field strength along the edges. Therefore, to enhance the approximation of the error we should use elements in the local problems which are zero on all edges since the error is mainly non-zero away from the edges. This corresponds to the technique in [9], Section 2.2 for elliptic problems and helps to localize the error equation.

Based on these requirements we use a finite dimensional space which is zero on all edges and for all faces we associate a basis function which is non-zero only on that face. In concrete terms, the finite element space  $V_h = \text{span}(\phi_j)$ ,  $j = 1, \dots, 9$ , on each element  $K$  is given by

$$(13) \quad \phi_j(x, y, z) = \phi_j^0(\xi, \eta, \zeta) \circ D_K^{-1}(x, y, z),$$

and  $\hat{V} = \text{span}(\phi_j^0)$ ,  $j = 1, 2, \dots, 9$ , where the face and the element bubble functions on the reference element  $\hat{K}$  are

$$\begin{aligned} \phi_1^0 &= ((1 - \xi)(1 - \eta)\eta(1 - \zeta)\zeta, 0, 0)^T, & \phi_6^0 &= (0, 0, (1 - \xi)\xi(1 - \eta)\eta\zeta)^T, \\ \phi_2^0 &= (\xi(1 - \eta)\eta(1 - \zeta)\zeta, 0, 0)^T, & \phi_7^0 &= ((1 - \xi)\xi(1 - \eta)\eta(1 - \zeta)\zeta, 0, 0)^T, \\ \phi_3^0 &= (0, (1 - \xi)\xi(1 - \eta)(1 - \zeta)\zeta, 0)^T, & \phi_8^0 &= (0, (1 - \xi)\xi(1 - \eta)\eta(1 - \zeta)\zeta, 0)^T, \\ \phi_4^0 &= (0, (1 - \xi)\xi\eta(1 - \zeta)\zeta, 0)^T, & \phi_9^0 &= (0, 0, (1 - \xi)\xi(1 - \eta)\eta(1 - \zeta)\zeta)^T, \\ \phi_5^0 &= (0, 0, (1 - \xi)\xi(1 - \eta)\eta(1 - \zeta))^T. \end{aligned}$$

Compared to (7) the transformation in (13) is a minor simplification which results in the same finite element space as the one in (7) but makes the computations slightly easier.

The analysis of the local problem given in Appendix A confirms that this basis results in a well posed problem for the discrete form of the error equation (11).

3.2.3. *Weak form of the local problem.* Using the approximation (12) and the local basis  $V_h$  we obtain the discrete form of (11): Find  $\hat{\mathbf{e}}_h \in V_h$  such that  $\forall \mathbf{w} \in V_h$

$$(14) \quad \begin{aligned} (\text{curl } \hat{\mathbf{e}}_h, \text{curl } \mathbf{w})_K - k^2(\hat{\mathbf{e}}_h, \mathbf{w})_K &= (\mathbf{J}_k, \mathbf{w})_K - (\text{curl } \mathbf{E}_h, \text{curl } \mathbf{w})_K \\ &+ k^2(\mathbf{E}_h, \mathbf{w})_K - \frac{1}{2}(\boldsymbol{\nu}_j \times (\text{curl } \mathbf{E}_h|_K + \text{curl } \mathbf{E}_h|_{K_j}), \mathbf{w})_{\partial K}. \end{aligned}$$

3.3. **Analysis of implicit error estimation.** Our objective is to solve the local problems arising in (14) for the unknown error term  $\hat{\mathbf{e}}_h$ . In this section, we establish that any reasonable approximation in (10) results in a well posed problem in (11). Observe that this equation is the variational form of the Maxwell equations equipped with natural boundary data. Note that a similar procedure for elliptic problems results in ill-posed local problems which require some postprocessing to be solvable [1].

3.3.1. *Lifting of the local problem.* The well-posedness of (11) will be investigated for the case of homogeneous natural boundary conditions. To do this we apply the trace lifting  $l : \text{Ran}(\gamma_\tau \circ \text{curl}|_{\partial K}) \rightarrow H(\text{curl}, K)$  (or equivalently, take an inverse of the tangential trace of the curl operator on  $H(\text{curl}, K)$ ) such that

$$\gamma_\tau(\text{curl } l\mathbf{u}) = \mathbf{u}, \quad \forall \mathbf{u} \in \text{Ran}(\gamma_\tau \circ \text{curl}|_{\partial K}).$$

Now defining  $\bar{\mathbf{e}}_h = \hat{\mathbf{e}}_h - l(\boldsymbol{\nu}_i \times \text{curl } \hat{\mathbf{e}}_h|_{\partial K})$  we can rewrite (11) as follows:

$$\begin{aligned} B_K(\bar{\mathbf{e}}_h, \mathbf{v}) &= B_K(\hat{\mathbf{e}}_h, \mathbf{v}) - B_K(l(\boldsymbol{\nu}_i \times \text{curl } \hat{\mathbf{e}}_h|_{\partial K}), \mathbf{v}) \\ &= (\mathbf{J}_k, \mathbf{v})_K - (\widehat{\gamma_\tau \text{curl } \mathbf{E}}, \pi_\tau \mathbf{v})_{\partial K} - B_K(\mathbf{E}_h, \mathbf{v}) \\ (15) \quad &- (\text{curl curl } l(\widehat{\gamma_\tau \text{curl } \mathbf{E}}), \mathbf{v})_K \\ &+ (\widehat{\gamma_\tau \text{curl } \mathbf{E}}, \pi_\tau \mathbf{v})_{\partial K} + k^2(l(\widehat{\gamma_\tau \text{curl } \mathbf{E}}), \mathbf{v}) \\ &= (\mathbf{J}_k - \text{curl curl } l(\widehat{\gamma_\tau \text{curl } \mathbf{E}}) + k^2l(\widehat{\gamma_\tau \text{curl } \mathbf{E}}), \mathbf{v})_K - B_K(\mathbf{E}_h, \mathbf{v}), \\ &\forall \mathbf{v} \in H(\text{curl}, K). \end{aligned}$$

Observe that on the right hand side we obtained a bounded linear functional of  $\mathbf{v}$  such that using the Riesz representation theorem we will denote it with  $(\tilde{\mathbf{J}}_k, \mathbf{v})_K$ . This approach is only necessary for our analysis; we do not need to compute the lifting operator explicitly, since in the finite element procedure the inhomogeneous natural boundary condition can be included in the variational form.

3.3.2. *Preliminaries to the well-posedness result.* In the following two subsections we prove some well-posedness results which are formulated in an arbitrary simply connected domain with a Lipschitz boundary. In this way, all of the results can also be applied in the case when local problems will be investigated in the subdomains of the original domain  $\Omega$ . Before proving the well-posedness of the variational problem we state a lemma which will be the cornerstone of our compactness arguments.

**Lemma 1.** *The Hilbert space  $H(\text{curl}, \Omega)$  can be decomposed as the direct sum of orthogonal subspaces:*

$$(16) \quad H(\text{curl}, \Omega) = \ker \text{curl} \oplus (\ker \text{curl})^\perp,$$

and the imbedding of the second component into  $[L_2(\Omega)]^3$  is compact.

*Proof.* Using the decomposition theorem in [13, p. 216] and the imbedding in Theorem 2.8 in [2], a standard argument gives the statement of the lemma. For a complete proof we refer to [19].  $\square$

3.3.3. *Well-posedness of the local problem.* We can state now the well-posedness of (15) and prove the following:

**Lemma 2.** *Assume that  $k$  is not a Maxwell eigenvalue in the sense that the problem: Find  $\mathbf{u} \in H(\text{curl}, \Omega)$  such that*

$$B(\mathbf{u}, \mathbf{v}) = 0, \quad \forall \mathbf{v} \in H(\text{curl}, \Omega)$$

*has only the trivial ( $\mathbf{u} = 0$ ) solution. Then the variational problem: Find  $\mathbf{u} \in H(\text{curl}, \Omega)$  such that*

$$(17) \quad B(\mathbf{u}, \mathbf{v}) = (\tilde{\mathbf{J}}_k, \mathbf{v}), \quad \forall \mathbf{v} \in H(\text{curl}, \Omega)$$

*has a unique solution for all  $\tilde{\mathbf{J}}_k \in [L_2(\Omega)]^3$ .*

*Proof.* The proof can be carried out using Lemma 1 and the technique in [21]. For a complete proof, we refer to [19].  $\square$

We should also prove that (at least) a smooth solution of the variational equation (17) in the lemma satisfies the homogeneous (natural) boundary condition, as well.

**Lemma 3.** *Assume that for the solution  $\mathbf{u}$  of (17)  $\text{curl curl } \mathbf{u} \in [L_2(\Omega)]^3$  holds. Then  $\mathbf{u}$  solves the Maxwell equation equipped with the natural boundary condition:*

$$(18) \quad \begin{aligned} \text{curl curl } \mathbf{u} - k^2 \mathbf{u} &= \tilde{\mathbf{J}}_k \quad \text{in } \Omega, \\ \boldsymbol{\nu} \times \text{curl } \mathbf{u} &= 0 \quad \text{on } \partial\Omega. \end{aligned}$$

*Proof.* Using the assumption in this lemma and the Green theorem (4) for the curl operator we obtain that

$$0 = (\text{curl } \mathbf{u}, \text{curl } \mathbf{v}) - k^2(\mathbf{u}, \mathbf{v}) - (\tilde{\mathbf{J}}_k, \mathbf{v}) = (\text{curl curl } \mathbf{u}, \mathbf{v}) - k^2(\mathbf{u}, \mathbf{v}) - (\tilde{\mathbf{J}}_k, \mathbf{v})$$

holds for every  $\mathbf{v} \in \mathcal{D}(\Omega)$  with  $\mathcal{D}(\Omega) = \{\mathbf{v} \in C^\infty(\Omega) : \mathbf{v} \text{ has compact support}\}$ . Since the embedding  $\mathcal{D}(\Omega) \subset H(\text{curl}, \Omega)$  is dense,  $(\text{curl curl } \mathbf{u} - k^2 \mathbf{u} - \tilde{\mathbf{J}}_k, \mathbf{v}) = 0$  for all  $\mathbf{v} \in H(\text{curl}, \Omega)$   $\text{curl curl } \mathbf{u} - k^2 \mathbf{u} = \tilde{\mathbf{J}}_k$  holds in  $[L_2(\Omega)]^3$ .

Using the Green theorem again we obtain that for all  $\mathbf{v} \in H(\text{curl}, \Omega)$

$$(19) \quad \begin{aligned} 0 &= (\text{curl curl } \mathbf{u} - k^2 \mathbf{u} - \tilde{\mathbf{J}}_k, \mathbf{v}) \\ &= (\text{curl } \mathbf{u}, \text{curl } \mathbf{v}) + (\gamma_\tau \text{curl } \mathbf{u}, \pi_\tau \mathbf{v})_{\partial\Omega} - k^2(\mathbf{u}, \mathbf{v}) - (\tilde{\mathbf{J}}_k, \mathbf{v}) \\ &= (\gamma_\tau \text{curl } \mathbf{u}, \pi_\tau \mathbf{v})_{\partial\Omega}. \end{aligned}$$

In this way, it also holds for any  $\mathbf{v} \in [H^1(\Omega)]^3$ , therefore, by the surjectivity of the trace mapping  $H^1(\Omega) \rightarrow H^{1/2}(\partial\Omega)$  we obtain that  $\gamma_\tau \text{curl } \mathbf{u} = 0$  in the  $[H^{-1/2}(\partial\Omega)]^3$  sense.  $\square$

*Remarks.* 1. Indeed, the dual space of the  $\pi_\tau$  map of  $H(\text{curl}, \Omega)$  is the kernel space of the natural boundary trace  $\gamma_\tau \circ \text{curl}$ . For the details, see [11].

2. As far as we consider a finite element scheme with piecewise polynomial basis functions, the eigenvalue problem in the weak sense (discussed in Lemma 3) is also equivalent with the eigenvalue problem for the original equation (1).

**3.4. The eigenvalue problem for the time-harmonic Maxwell equations with natural boundary conditions.** The well posedness of the local problems for the error can be guaranteed if we ensure that  $k$  is not a Maxwell eigenvalue of these problems.

More specifically, recall that in Section 2, the weak form (9) for the local error equation equipped with the natural boundary condition (12) results in the variational problem (15) which is well posed by Lemma 2 if and only if  $k$  is not an eigenvalue of the appropriate boundary value problem (18). In this section, we determine the eigenvalues belonging to cubic subdomains. In this way, for any  $k$  (given in the original problem (1)) we will be able to choose the subdomain  $K$  in the tessellation such that the boundary value problem (9) (or even (11)) on  $K$  will be well posed.

First, we reduce the eigenvalue problem such that we can apply some techniques and results which are available for the Laplacian operator.



**Lemma 4.** *If  $k \neq 0$  is a Maxwell eigenvalue of the differential operator on the left hand side of (18), then its eigenfunction  $\mathbf{u}$  is in the subspace  $\mathbf{u} \in (\ker \operatorname{curl})^\perp$  and solves the following Helmholtz equation:*

$$(20) \quad \begin{aligned} \Delta \mathbf{u} - k^2 \mathbf{u} &= 0 \quad \text{in } \Omega, \\ \boldsymbol{\nu} \times \operatorname{curl} \mathbf{u} &= 0 \quad \text{on } \partial\Omega, \end{aligned}$$

where the operator  $\Delta$  is defined componentwise: for  $\mathbf{v} : \Omega \rightarrow \mathbb{R}^3$  with  $\mathbf{v} = (v_1, v_2, v_3)$ ,  $\Delta \mathbf{v} := (\Delta v_1, \Delta v_2, \Delta v_3)$ .

*Proof.* Assume that  $\mathbf{u} = \mathbf{u}_1 + \mathbf{u}_2$  (according to the decomposition (16)) is an eigenfunction of (18). Then

$$(21) \quad \operatorname{curl} \operatorname{curl}(\mathbf{u}_1 + \mathbf{u}_2) - k^2(\mathbf{u}_1 + \mathbf{u}_2) = \operatorname{curl} \operatorname{curl} \mathbf{u}_2 - k^2(\mathbf{u}_1 + \mathbf{u}_2) = 0.$$

Note that the boundary condition  $\boldsymbol{\nu} \times \operatorname{curl} \mathbf{u} = 0$  implies that  $\boldsymbol{\nu} \times \operatorname{curl} \mathbf{u}_2 = 0$  and therefore, taking the  $[L_2(\Omega)]^3$  scalar product of both sides with  $\mathbf{u}_1$  and using the orthogonality in (16), we obtain

$$\begin{aligned} 0 &= (\operatorname{curl} \operatorname{curl} \mathbf{u}_2 - k^2(\mathbf{u}_1 + \mathbf{u}_2), \mathbf{u}_1) \\ &= (\operatorname{curl} \mathbf{u}_2, \operatorname{curl} \mathbf{u}_1) + (\gamma_\tau \operatorname{curl} \mathbf{u}_2, \pi_\tau \mathbf{u}_1)_{\partial\Omega} - k^2(\mathbf{u}_1, \mathbf{u}_1) = -k^2 \|\mathbf{u}_1\|^2. \end{aligned}$$

This means that  $\mathbf{u}_1 = 0$ , and using the relation  $\operatorname{curl} \operatorname{curl} \mathbf{u}_2 = -\Delta \mathbf{u}_2 + \operatorname{grad} \operatorname{div} \mathbf{u}_2 = -\Delta \mathbf{u}_2$  in (21) we obtain the statement in the lemma.  $\square$

In the following we use the conditions arising from the fact that  $\mathbf{u} \in (\ker \operatorname{curl})^\perp \subset H_0(\operatorname{div} 0, \Omega)$  (see proof of Lemma 1) and the boundary condition in (20):

$$(22) \quad \operatorname{div} \mathbf{u} = 0 \quad \text{in } \Omega,$$

$$(23) \quad \mathbf{u} \cdot \boldsymbol{\nu} = 0 \quad \text{on } \partial\Omega,$$

$$(24) \quad \boldsymbol{\nu} \times \operatorname{curl} \mathbf{u} = 0 \quad \text{on } \partial\Omega.$$

Accordingly, our objective is to find the eigenvalues and eigenfunctions of the following operator  $\mathcal{L}$ :

$$(25) \quad \begin{aligned} \mathcal{L} : [L_2(\Omega)]^3 &\rightarrow [L_2(\Omega)]^3, \\ \operatorname{Dom} \mathcal{L} &= \{\mathbf{u} \in H_0(\operatorname{div} 0, \Omega) : \Delta \mathbf{u} \in [L_2(\Omega)]^3 \text{ and } \boldsymbol{\nu} \times \operatorname{curl} \mathbf{u} = 0 \text{ on } \partial\Omega\}, \\ \mathcal{L} \mathbf{u} &= \Delta \mathbf{u}. \end{aligned}$$

**3.5. Eigenvalues in a rectangular domain.** In this subsection, we investigate the eigenvalue problem on the cube  $\Omega = (0, \pi) \times (0, \pi) \times (0, \pi)$ . Applying a linear transformation for the eigenfunctions on  $\Omega$  allows us to solve the eigenvalue problem on rectangular domains.

This result makes it possible to choose the subdomains in the finite element tessellation in such a way that the local problem for the error is well posed on each subdomain.

We present only the results in this section; the proofs are provided in [19].

**Theorem 1.** *The eigenfunctions of  $\mathcal{L}$  defined in (25) are given by:*

$$(26) \quad \mathbf{u}(x_1, x_2, x_3) = \begin{pmatrix} C_1 \sin k_1 x_1 \cos k_2 x_2 \cos k_3 x_3 \\ C_2 \cos k_1 x_1 \sin k_2 x_2 \cos k_3 x_3 \\ C_3 \cos k_1 x_1 \cos k_2 x_2 \sin k_3 x_3 \end{pmatrix},$$

for any  $k_1, k_2, k_3 \in \mathbb{N}$  with

$$(27) \quad k_1 C_1 + k_2 C_2 + k_3 C_3 = 0 \quad \text{and} \quad C_1, C_2, C_3 \in \mathbb{R}.$$

Based on Theorem 1 we can give the eigenfunctions and eigenvalues of the Maxwell eigenvalue problem with homogeneous natural boundary conditions

$$(28) \quad \begin{aligned} \operatorname{curl} \operatorname{curl} \mathbf{v} &= k^2 \mathbf{v} \quad \text{in } B_{a,b,c}, \\ \boldsymbol{\nu} \times \operatorname{curl} \mathbf{v} &= 0 \quad \text{on } \partial B_{a,b,c}, \end{aligned}$$

where  $B_{a,b,c}$  is a rectangular domain with edge lengths  $a, b$  and  $c$ , respectively.

**Theorem 2.** *The eigenfunctions of the Maxwell equation (28) are*

$$\mathbf{v}(x, y, z) = \begin{pmatrix} C_1 \sin \frac{k_1 \pi}{a} x \cos \frac{k_2 \pi}{b} y \cos \frac{k_3 \pi}{c} z \\ C_2 \cos \frac{k_1 \pi}{a} x \sin \frac{k_2 \pi}{b} y \cos \frac{k_3 \pi}{c} z \\ C_3 \cos \frac{k_1 \pi}{a} x \cos \frac{k_2 \pi}{b} y \sin \frac{k_3 \pi}{c} z \end{pmatrix},$$

for any  $k_1, k_2, k_3 \in \mathbb{N}$  with

$$\frac{k_1 \pi}{a} C_1 + \frac{k_2 \pi}{b} C_2 + \frac{k_3 \pi}{c} C_3 = 0 \quad \text{and} \quad C_1, C_2, C_3 \in \mathbb{R}$$

and the appropriate eigenvalues are  $k^2 = \left(\frac{k_1 \pi}{a}\right)^2 + \left(\frac{k_2 \pi}{b}\right)^2 + \left(\frac{k_3 \pi}{c}\right)^2$  with  $k_1, k_2, k_3 \in \mathbb{N}$  arbitrary.

#### 4. IMPLICIT ERROR ESTIMATE AS A LOWER BOUND OF THE ERROR

If the a posteriori error estimates have to be used in an adaptation procedure we also have to investigate a lower bound for the exact error. This will ensure that we do not get a pessimistic overestimate of the actual error when the mesh size is reduced. For the estimates in this section we will define an *error indicator*  $\eta_K$  on  $K$ . Our analysis consists of two steps: first, we point out that the implicit a posteriori error estimate  $\hat{e}_h$  discussed in this paper provides a lower bound estimate of  $\eta_K$  (up to a certain factor). Second, we verify that the error indicator can also be used as a lower bound (up to a certain factor and some computable remainders) of the exact error on a patch of the subdomain  $K$ . The proof is based on the approach in [1]. While the second step is a rather straightforward modification of the original proof for elliptic problems, the first one needs a more careful analysis since the bilinear form  $B$  in the variational problem is not coercive.

Since the mappings  $D_K$  are affine, the subdomains in the tessellation  $\mathcal{T}_h$  consist of parallelepipeds. Moreover, we assume that the mesh is non-degenerated, i.e. the ratio of the diameter of elements and their minimal edge length  $\frac{\operatorname{diam} K}{\min |e_K|}$  is bounded. An important consequence of this assumption is that there are constants  $K_1, K_2 \in \mathbb{R}^+$  such that for any  $K$  with  $\max |e_k| < h$  we have

$$(29) \quad K_1 h \leq \min \operatorname{eig} dD_K \leq \max \operatorname{eig} dD_K \leq K_2 h,$$

where  $\operatorname{eig}$  denotes the spectrum. Since the mapping  $D_K$  is affine,  $dD_K$  is the linear part of  $D_K$ .

For solving the local problem for the error we use the finite dimensional space  $V_h$  on  $K$ . This choice should lead to a well posed local problem. A necessary condition for this is given in Lemma 8.

In the finite element discretization we use the notation  $\boldsymbol{\nu} \times \cdot$  instead of  $\gamma_\tau$ , and similarly, for functions  $\mathbf{v} \in [H^1(K)]^3$  we may omit the operator  $\pi_\tau$  on the boundary making a closer link to the numerical procedure. For the consecutive computations we also recall a Green's formula according to (4) which states that

for all  $\mathbf{u} \in H(\text{curl}, \Omega)$  and  $\mathbf{v} \in [H^1(\Omega)]^3$  the following identity holds (Theorem 3.29 in [21]):

$$(30) \quad (\text{curl } \mathbf{u}, \mathbf{v}) - (\mathbf{u}, \text{curl } \mathbf{v}) = (\boldsymbol{\nu} \times \mathbf{u}, \mathbf{v})_{\partial\Omega}.$$

Using (9) and the approximation (12) we obtain the weak form for the error estimate  $\hat{\mathbf{e}}_h$  on the bubble function space  $V_h$  (introduced in Section 3.2.2) as follows: Find an  $\hat{\mathbf{e}}_h \in V_h$ , such that  $\forall \mathbf{v} \in V_h$  the following relation is satisfied:

$$(31) \quad \begin{aligned} B_K(\hat{\mathbf{e}}_h, \mathbf{v}) &= (\mathbf{J}_k, \mathbf{v})_K - B_K(\mathbf{E}_h, \mathbf{v}) - \frac{1}{2} \sum_j (\boldsymbol{\nu}_j \times [\text{curl } \mathbf{E}_h|_K + \text{curl } \mathbf{E}_h|_{K_j}], \mathbf{v})_{l_j} \\ &= (\mathbf{J}_k, \mathbf{v})_K - (\text{curl curl } \mathbf{E}_h, \mathbf{v})_K + k^2(\mathbf{E}_h, \mathbf{v})_K + (\boldsymbol{\nu} \times \text{curl } \mathbf{E}_h, \mathbf{v})_{\partial K} \\ &\quad - \frac{1}{2} \sum_j (\boldsymbol{\nu}_j \times [\text{curl } \mathbf{E}_h|_K + \text{curl } \mathbf{E}_h|_{K_j}], \mathbf{v})_{l_j} \\ &= (\mathbf{J}_k, \mathbf{v})_K - (\text{curl curl } \mathbf{E}_h, \mathbf{v})_K + k^2(\mathbf{E}_h, \mathbf{v})_K \\ &\quad + \frac{1}{2} \sum_j (\boldsymbol{\nu}_j \times [\text{curl } \mathbf{E}_h|_K - \text{curl } \mathbf{E}_h|_{K_j}], \mathbf{v})_{l_j} \\ &= (\mathbf{r}_K, \mathbf{v})_K + \sum_j (\mathbf{R}_{l_j}, \mathbf{v})_{l_j}, \end{aligned}$$

where we have used the notations

$$\mathbf{r}_K = \mathbf{J}_k - \text{curl curl } \mathbf{E}_h + k^2 \mathbf{E}_h \quad \text{in } K$$

for the residual within the subdomain  $K$  and

$$\mathbf{R}_{l_j} = \frac{1}{2}(\boldsymbol{\nu}_j \times [\text{curl } \mathbf{E}_h|_K - \text{curl } \mathbf{E}_h|_{K_j}])$$

for the tangential jump of the curl at  $l_j$  within the subdomain  $K$  and where  $\hat{\mathbf{e}}_h$  denotes the desired implicit error estimate. Note that (31) gives a variational form for  $\hat{\mathbf{e}}_h$  which includes the approximation in (12). In the following we drop the subscript for the residual and the tangential jump, respectively, the localization will be shown when taking the norm (or some bilinear map) of these quantities.

Using the above quantities  $\mathbf{r}$  and  $\mathbf{R}$  we define  $\eta_K$  as an error indicator as follows:

$$\eta_K = (h^2 \|\mathbf{r}\|_{[L_2(K)]^3}^2 + h \|\mathbf{R}\|_{[L_2(\partial K)]^3}^2)^{\frac{1}{2}}.$$

**4.1. Bubble functions.** For the analysis we use the bubble function technique outlined in [1] and recall some basic definitions:

**Definition 1.** Let  $\hat{\Psi} : \hat{K} \rightarrow \mathbb{R}$  be given by

$$\hat{\Psi}(\xi, \eta, \zeta) = \xi(1 - \xi)\eta(1 - \eta)\zeta(1 - \zeta)$$

and  $\Psi : K \rightarrow \mathbb{R}$  defined using the isoparametric mapping  $D_K$ . Similarly, for a given  $\hat{\mathbf{p}} \in \hat{P}$  where  $\hat{P} \subset [\mathcal{P}^1(\hat{K})]^3$ , with  $\mathcal{P}^1(\hat{K})$  a finite dimensional space of polynomials, an appropriate  $\mathbf{p} \in P \subset [\mathcal{P}^1(K)]^3$  can be defined by  $\mathbf{p}(\mathbf{x}) = \hat{\mathbf{p}}(D_K^{-1}(\mathbf{x}))$ .

In the error estimation process we substitute  $\mathbf{v} \in P$  with  $\Psi \mathbf{v}$  on  $K$ , where  $\Psi \mathbf{v}$  can be extended by continuity to  $\partial K$ . The following lemmas ensure that the multiplication with  $\Psi$  does not influence the magnitude of the  $L_2$  or the curl norm compared to that of  $\mathbf{v}$ . The proofs are based on scaling arguments.

**Lemma 5.** *Consider a non-degenerate family  $\mathcal{T}_h$  of parallelepiped meshes on  $\Omega$ . Then there exists a positive constant  $C$  such that for all subdomains  $K \subset \mathcal{T}_h$  and  $\mathbf{p} \in P$*

$$(32) \quad C^{-1} \|\mathbf{p}\|_{[L_2(K)]^3}^2 \leq (\Psi \mathbf{p}, \mathbf{p})_K \leq C \|\mathbf{p}\|_{[L_2(K)]^3}^2$$

and

$$(33) \quad C^{-1} \|\mathbf{p}\|_{[L_2(K)]^3}^2 \leq \|\Psi \mathbf{p}\|_{[L_2(K)]^3}^2 + h^2 \|\operatorname{curl} \Psi \mathbf{p}\|_{[L_2(K)]^3}^2 \leq C \|\mathbf{p}\|_{[L_2(K)]^3}^2,$$

with  $h$  the diameter of  $K$ .

**Definition 2.** According to [1, p. 24] we define the face bubble functions  $\hat{\Phi}_j : \hat{K} \rightarrow \mathbb{R}, j = 1, \dots, 6$ , which vanish on all edges of  $\hat{K}$  and all faces  $\hat{l}_m, m = 1, \dots, 6, m \neq j$ .

Using the mapping  $D_K : \hat{K} \rightarrow K$  we define  $\Phi_j, j = 1, \dots, 6$ , the bubble functions associated with the faces  $l_j$  of  $K \in \mathcal{T}_h$ .

We localize a face bubble function  $\Phi_i$ , associated to the face  $l_i$ , by restricting it to the subdomain  $\tilde{K}_i = K \cup l_i \cup K_i$ , where  $l_i$  is the common face of  $K$  and  $K_i$ . For the consecutive estimates we again provide some inequalities:

**Lemma 6.** *Let us consider a non-degenerate family  $\mathcal{T}_h$  of parallelepiped elements on  $\Omega$ . Then there exists a positive constant  $C$  such that for all subdomains  $K \subset \mathcal{T}_h$ , functions  $\mathbf{p} \in P$  (where  $P$  is a fixed finite dimensional subspace of  $[L_2(K)]^3$ ) and faces  $l_i, i = 1, \dots, 6$ , the following inequalities hold:*

$$(34) \quad C^{-1} \|\mathbf{p}\|_{[L_2(l_i)]^3}^2 \leq \int_{l_i} \Phi_i \mathbf{p} \cdot \mathbf{p} \leq C \|\mathbf{p}\|_{[L_2(l_i)]^3}^2,$$

$$(35) \quad \|\Phi_i \mathbf{p}\|_{[L_2(\tilde{K}_i)]^3}^2 \leq Ch \|\mathbf{p}\|_{[L_2(l_i)]^3}^2,$$

$$(36) \quad \|\Phi_i \mathbf{p}\|_{[L_2(l_i)]^3}^2 \leq C \|\mathbf{p}\|_{[L_2(l_i)]^3}^2,$$

$$(37) \quad \|\Phi_i \mathbf{p}\|_{\operatorname{curl}, \tilde{K}_i}^2 \leq Ch^{-1} \|\mathbf{p}\|_{[L_2(l_i)]^3}^2.$$

*Proof.* The proof can be carried out again using scaling arguments similar to Theorem 2.4 in [1] using the fact that the mesh is non-degenerate.  $\square$

We also state a lemma on the comparison of the different norms in the finite element spaces when they are given on a scale of cubes.

**Lemma 7.** *For all subdomains  $K \subset \mathcal{T}_h$  (with the faces  $l_i, i = 1, \dots, 6$ ) and for all  $\mathbf{v} \in V_h$  we have the estimates*

$$(38) \quad \|\mathbf{v}_k\|_{[L_2(K)]^3} \leq Ch \|\operatorname{curl} \mathbf{v}_k\|_{[L_2(K)]^3}$$

and

$$(39) \quad \|\mathbf{v}_k\|_{[L_2(l_i)]^3} \leq Ch^{\frac{1}{2}} \|\operatorname{curl} \mathbf{v}_k\|_{[L_2(K)]^3}$$

with a constant  $C$  which does not depend on  $h$ .

*Proof.* The proof can be carried out with a change of variables according to  $D_K$ .  $\square$

**4.2. Lower bound for the computational error in terms of the residuals.**

When the bilinear form  $B$  is restricted to  $\hat{V} \times \hat{V}$  we may identify it with the stiffness matrix  $B_1$ , which is given as  $B_1 = B_{1,\text{curl}} - k^2 B_{1,0}$  such that the  $(i, j)$ th entries  $i, j = 1, 2, \dots, n$  are as follows:

$$B_{1,\text{curl}}[i][j] = (\text{curl } \hat{\Phi}_i^*, \text{curl } \hat{\Phi}_j^*)_{\hat{K}}, \quad B_{1,0}[i][j] = (\hat{\Phi}_i^*, \hat{\Phi}_j^*)_{\hat{K}}$$

with a basis  $\{\hat{\Phi}_i^*\}_{i=1}^n$  of  $\hat{V}$ .  $B_{1,K}$  denotes the appropriate mass matrix on  $K$  which can be again decomposed as

$$B_{1,K} = B_{1,\text{curl},K} - k^2 B_{1,0,K},$$

where the components are defined as

$$B_{1,\text{curl},K}(\Phi_i^*, \Phi_j^*) = (\text{curl } \Phi_i^*, \text{curl } \Phi_j^*)_K \quad \text{and} \quad B_{1,0,K}(\Phi_i^*, \Phi_j^*) = (\Phi_i^*, \Phi_j^*)_K$$

with an appropriate basis  $\{\Phi_i^*\}_{i=1}^n$  of  $V_h$ .

We can state now the following lemma, which is central in our analysis.

**Lemma 8.** *Assume that  $\mathcal{T}_h$  is a cubic mesh. Then for a sufficiently fine mesh the bilinear form  $B_K$  satisfies the discrete inf-sup condition uniformly on  $V_h \times V_h$ , namely there is positive  $h_0$  and a constant  $C_0 > 0$  such that for any  $0 < h < h_0$*

$$(40) \quad C_0 \sup_{\mathbf{v} \in V_h} \frac{B_K(\mathbf{u}, \mathbf{v})}{\|\mathbf{v}\|_{\text{curl},K}} \geq \|\mathbf{u}\|_{\text{curl},K}, \quad \forall \mathbf{u} \in V_h,$$

where  $K$  is the cube with edge length  $h$  and  $C_0$  does not depend on  $h$ .

The proof of Lemma 8 is given in Appendix A.

**Lemma 9.** *If we choose the bubble function space  $V_h$  and consider a cubic tessellation, then the bilinear form for the error on  $K = (0, h)^3$  reads as  $B_{1,K} = \frac{1}{h} B_{1,\text{curl}} - k^2 h B_{1,0}$  and the mesh size  $h_0$  can be taken as*

$$h_0 = \frac{20(16 - \sqrt{246})}{\sqrt{2k^2 + 1}(16 + \sqrt{246})}$$

in Lemma 8.

It is easy to see that  $B_K$  is continuous on the whole of  $H(\text{curl}, K) \times H(\text{curl}, K)$  as stated in the following lemma.

**Lemma 10.** *For the bilinear form  $B_K$  we have the continuity estimate:*

$$(41) \quad |B_K(\mathbf{u}, \mathbf{v})| \leq \sqrt{2}(1 + k^2) \|\mathbf{u}\|_{\text{curl},K} \|\mathbf{v}\|_{\text{curl},K}, \quad \forall \mathbf{u}, \mathbf{v} \in H(\text{curl}, K).$$

*Proof.* We prove the lemma with a straightforward computation as follows:

$$\begin{aligned} |B_K(\mathbf{u}, \mathbf{v})|^2 &= |(\text{curl } \mathbf{u}, \text{curl } \mathbf{v})_K - k^2(\mathbf{u}, \mathbf{v})_K|^2 \\ &\leq 2(\text{curl } \mathbf{u}, \text{curl } \mathbf{v})_K^2 + 2k^4(\mathbf{u}, \mathbf{v})_K^2 \\ &\leq 2\|\text{curl } \mathbf{u}\|_{[L_2(K)]^3}^2 \|\text{curl } \mathbf{v}\|_{[L_2(K)]^3}^2 + 2k^4\|\mathbf{u}\|_{[L_2(K)]^3}^2 \|\mathbf{v}\|_{[L_2(K)]^3}^2 \\ &\leq 2(1 + k^4)\|\mathbf{u}\|_{\text{curl},K}^2 \|\mathbf{v}\|_{\text{curl},K}^2. \end{aligned}$$

Taking the square roots on both sides we obtain the estimate in the lemma.  $\square$

We now compare the error indicator  $\eta_K$  with the implicit error estimate  $\hat{e}_h$  obtained from the weak form (31) and state the following lemma.

**Lemma 11.** *There is a constant  $C_1$  independent from the mesh parameter  $h$  such that*

$$(42) \quad \|\hat{e}_h\|_{\text{curl},K} \leq C_1 \eta_K,$$

where  $\hat{e}_h$  is the implicit error estimate on the subdomain  $K$ .

*Proof.* Using the weak form (31) we obtain

$$(43) \quad \begin{aligned} \|\hat{e}_h\|_{\text{curl},K} &\leq C_0 \sup_{\mathbf{v} \in V_h} \frac{B_K(\hat{e}_h, \mathbf{v})}{\|\mathbf{v}\|_{\text{curl},K}} = C_0 \sup_{\mathbf{v} \in V_h} \frac{(\mathbf{r}, \mathbf{v})_K + (\mathbf{R}, \mathbf{v})_{\partial K}}{\|\mathbf{v}\|_{\text{curl},K}} \\ &\leq C_0 \sup_{\mathbf{v} \in V_h} \frac{1}{\|\mathbf{v}\|_{\text{curl},K}} (\|\mathbf{r}\|_{[L_2(K)]^3} \|\mathbf{v}\|_{[L_2(K)]^3} \\ &\quad + \|\mathbf{R}\|_{[L_2(\partial K)]^3} \|\mathbf{v}\|_{[L_2(\partial K)]^3}) \\ &\leq C \cdot C_0 h \|\mathbf{r}\|_{[L_2(K)]^3} + h^{\frac{1}{2}} \|\mathbf{R}\|_{[L_2(\partial K)]^3} \leq C \cdot C_0 \sqrt{2} \eta_K. \end{aligned}$$

In the first inequality we used (40), then the weak formulation (31) followed by the Cauchy-Schwarz inequality. Finally, we applied the estimates (38) and (39) and a basic inequality.  $\square$

Note that the error estimate  $\hat{e}_h$  in Lemma 11 gives the exact error (according to the weak form (31)) assuming that the boundary condition (12) is exact. In the following we will compute an approximation of  $\hat{e}_h$  in the finite element space  $V_h$ .

The upper estimate of the error indicator  $\eta_K$  will be obtained using the bubble function technique [1]. We first provide a variational form for the exact error  $e_h$  based on the third line of (9) and using the notations of the previous sections:

$$(44) \quad \begin{aligned} B(e_h, \mathbf{v}) &= (\mathbf{J}_k, \mathbf{v}) - ((\text{curl } \mathbf{E}_h, \text{curl } \mathbf{v}) - k^2(\mathbf{E}_h, \mathbf{v})) \\ &= \sum_{K \in \mathcal{T}_h} \{(\mathbf{J}_k, \mathbf{v})_K - (\text{curl curl } \mathbf{E}_h - k^2 \mathbf{E}_h, \mathbf{v})_K \\ &\quad + \sum_j (\boldsymbol{\nu}_j \times \text{curl } \mathbf{E}_h, \pi_\tau \mathbf{v})_{l_j}\} \\ &= \sum_{K \in \mathcal{T}_h} (\mathbf{r}, \mathbf{v})_K + \sum_\gamma (\mathbf{R}, \mathbf{v})_\gamma, \quad \forall \mathbf{v} \in H(\text{curl}, \Omega), \end{aligned}$$

where the last sum is taken over all of the interelement faces  $\gamma$  inside of  $\Omega$ . To obtain the second line in (44) we used the perfect conducting boundary condition on  $\partial\Omega$ , while the final expression was obtained by summation of the components of a given face from the both sides. This expression can also be related with (31); on the whole domain  $\Omega$ , the variational form for the exact and the estimated error coincide since the boundary conditions are given.

We will choose  $\mathbf{v}$  in (44) using the bubble function technique such that the boundary integral vanishes, which will result in a lower bound for the error on each subdomain depending only on the element residual  $\mathbf{r}$  in the subdomain  $K$ . It is also important that the choice for  $\mathbf{v}$  is suitable for the estimates (32)-(33), which only apply in a finite dimensional space. In light of this, we denote by  $\bar{\mathbf{r}}$  the elementwise interpolation of the residual  $\mathbf{r}$  using the function space  $V_h$  and choose  $\mathbf{v} = \Psi_K \bar{\mathbf{r}}$  on each subdomain  $K$  and zero elsewhere. Inserting this choice for  $\mathbf{v}$  into (44) gives that

$$(45) \quad B(e_h, \Psi_K \bar{\mathbf{r}}) = (\mathbf{r}, \Psi_K \bar{\mathbf{r}})_K.$$

In the following estimates we use  $C$  for a generic constant independent of the mesh size  $h$  and frequency  $k$ , which can be different in each formula. Using (45), and inequalities (32), (33) for  $h \leq 1$  we obtain the following estimate:

$$\begin{aligned}
 (46) \quad \|\bar{\mathbf{r}}\|_{[L_2(K)]^3}^2 &\leq C(\Psi_K \bar{\mathbf{r}}, \bar{\mathbf{r}})_K = C((\Psi_K \bar{\mathbf{r}}, \bar{\mathbf{r}} - \mathbf{r})_K + B(\mathbf{e}_h, \Psi_K \bar{\mathbf{r}})) \\
 &\leq C(\|\Psi_K \bar{\mathbf{r}}\|_{[L_2(K)]^3} \|\bar{\mathbf{r}} - \mathbf{r}\|_{[L_2(K)]^3} + (1 + k^2)\|\mathbf{e}_h\|_{\text{curl},K} \|\Psi_K \bar{\mathbf{r}}\|_{\text{curl},K}) \\
 &\leq C(\|\bar{\mathbf{r}}\|_{[L_2(K)]^3} \|\bar{\mathbf{r}} - \mathbf{r}\|_{[L_2(K)]^3} + (1 + k^2)h^{-1}\|\mathbf{e}_h\|_{\text{curl},K}) \|\bar{\mathbf{r}}\|_{[L_2(K)]^3}.
 \end{aligned}$$

Dividing by  $\|\bar{\mathbf{r}}\|_{[L_2(K)]^3}$  and using the triangle inequality we finally obtain that

$$\begin{aligned}
 (47) \quad \|\mathbf{r}\|_{[L_2(K)]^3} &\leq \|\bar{\mathbf{r}}\|_{[L_2(K)]^3} + \|\mathbf{r} - \bar{\mathbf{r}}\|_{[L_2(K)]^3} \\
 &\leq C(\|\bar{\mathbf{r}} - \mathbf{r}\|_{[L_2(K)]^3} + (1 + k^2)h^{-1}\|\mathbf{e}_h\|_{\text{curl},K}).
 \end{aligned}$$

We proceed similarly for the boundary jumps and denote by  $\bar{\mathbf{R}}$  the approximation of the boundary jump using the trace of  $V_h$  on the element boundaries, which is then defined on the interelement faces  $l_i$ . The error arising from these terms can be localized on  $\tilde{K}$  by the choice:

$$\mathbf{v} = \Phi_l \bar{\mathbf{R}},$$

associated to the face  $l$  as in Lemma 6 which is again extended (preserving the continuity) to be zero outside of  $\tilde{K}$ . This leads us to the identity

$$(48) \quad (\Phi_l \bar{\mathbf{R}}, \mathbf{R})_l = B_{\tilde{K}}(\mathbf{e}_h, \Phi_l \bar{\mathbf{R}}) - (\Phi_l \bar{\mathbf{R}}, \mathbf{r})_{\tilde{K}}.$$

Using then (48), the Cauchy–Schwarz inequality and inequalities (34), (35), (36), and (37) we obtain the following estimate:

$$\begin{aligned}
 (49) \quad \|\bar{\mathbf{R}}\|_{[L_2(l)]^3}^2 &\leq C(\Phi_l \bar{\mathbf{R}}, \bar{\mathbf{R}})_l = C(\Phi_l \bar{\mathbf{R}}, \bar{\mathbf{R}} - \mathbf{R})_l + C(\Phi_l \bar{\mathbf{R}}, \mathbf{R})_l \\
 &= C((\Phi_l \bar{\mathbf{R}}, \bar{\mathbf{R}} - \mathbf{R})_l + B_{\tilde{K}}(\mathbf{e}_h, \Phi_l \bar{\mathbf{R}}) - (\Phi_l \bar{\mathbf{R}}, \mathbf{r})_{\tilde{K}}) \\
 &\leq C(\|\Phi_l \bar{\mathbf{R}}\|_{[L_2(l)]^3} \|\bar{\mathbf{R}} - \mathbf{R}\|_{[L_2(l)]^3} \\
 &\quad + \sqrt{2}(1 + k^2)\|\mathbf{e}_h\|_{\text{curl},\tilde{K}} \|\Phi_l \bar{\mathbf{R}}\|_{\text{curl},\tilde{K}} + \|\Phi_l \bar{\mathbf{R}}\|_{[L_2(\tilde{K})]^3} \|\mathbf{r}\|_{[L_2(\tilde{K})]^3}) \\
 &\leq C(\|\bar{\mathbf{R}}\|_{[L_2(l)]^3} \|\bar{\mathbf{R}} - \mathbf{R}\|_{[L_2(l)]^3} \\
 &\quad + h^{-\frac{1}{2}}(1 + k^2)\|\mathbf{e}_h\|_{\text{curl},\tilde{K}} \|\bar{\mathbf{R}}\|_{[L_2(l)]^3} + h^{\frac{1}{2}}\|\bar{\mathbf{R}}\|_{[L_2(l)]^3} \|\mathbf{r}\|_{[L_2(\tilde{K})]^3}),
 \end{aligned}$$

which after division by  $\|\bar{\mathbf{R}}\|_{[L_2(l)]^3}$ , yields

$$(50) \quad \|\bar{\mathbf{R}}\|_{[L_2(l)]^3} \leq C(\|\bar{\mathbf{R}} - \mathbf{R}\|_{[L_2(l)]^3} + h^{-\frac{1}{2}}(1 + k^2)\|\mathbf{e}_h\|_{\text{curl},\tilde{K}} + h^{\frac{1}{2}}\|\mathbf{r}\|_{[L_2(\tilde{K})]^3}).$$

Finally, adding  $\|\bar{\mathbf{R}} - \mathbf{R}\|_{[L_2(l)]^3}$  to both sides results in the estimate

$$\begin{aligned}
 (51) \quad \|\mathbf{R}\|_{[L_2(l)]^3} &\leq \|\bar{\mathbf{R}}\|_{[L_2(l)]^3} + \|\mathbf{R} - \bar{\mathbf{R}}\|_{[L_2(l)]^3} \\
 &\leq C(\|\bar{\mathbf{R}} - \mathbf{R}\|_{[L_2(l)]^3} + h^{-\frac{1}{2}}(1 + k^2)\|\mathbf{e}_h\|_{\text{curl},\tilde{K}} + h^{\frac{1}{2}}\|\mathbf{r}\|_{[L_2(\tilde{K})]^3}).
 \end{aligned}$$

Using (47) we obtain that

$$\begin{aligned}
 (52) \quad \|\mathbf{R}\|_{[L_2(l)]^3} &\leq C(h^{-\frac{1}{2}}(1 + k^2)\|\mathbf{e}_h\|_{\text{curl},\tilde{K}} \\
 &\quad + h^{\frac{1}{2}}\|\bar{\mathbf{r}} - \mathbf{r}\|_{[L_2(\tilde{K})]^3} + \|\bar{\mathbf{R}} - \mathbf{R}\|_{[L_2(l)]^3}).
 \end{aligned}$$

Taking the square of (52) and (47) respectively, we obtain:

$$(53) \quad \begin{aligned} \|\mathbf{R}\|_{[L_2(l)]^3}^2 &\leq C(h^{-1}(1+k^2)^2\|e_h\|_{\text{curl},\tilde{K}}^2 \\ &\quad + h\|\bar{\mathbf{r}} - \mathbf{r}\|_{[L_2(\tilde{K})]^3}^2 + \|\bar{\mathbf{R}} - \mathbf{R}\|_{[L_2(l)]^3}^2) \end{aligned}$$

and

$$(54) \quad \|\mathbf{r}\|_{[L_2(K)]^3}^2 \leq C(\|\bar{\mathbf{r}} - \mathbf{r}\|_{[L_2(K)]^3}^2 + (1+k^2)^2h^{-2}\|e_h\|_{\text{curl},K}^2).$$

Using the obvious equality

$$\|\mathbf{R}\|_{[L_2(\partial K)]^3}^2 = \sum_{j=1}^6 \|\mathbf{R}\|_{[L_2(l_j)]^3}^2$$

we sum up (53) for all faces  $l_j$  of  $K$  and multiply  $\|\mathbf{r}\|_{[L_2(K)]^3}^2$  with  $h^2$  and  $\|\mathbf{R}\|_{[L_2(\partial K)]^3}^2$  with  $h$ , respectively. Using the definition of  $\eta_K$  we finally get the estimate:

$$(55) \quad \begin{aligned} \frac{1}{C}\eta_K^2 &\leq h^2\|\bar{\mathbf{r}} - \mathbf{r}\|_{[L_2(\tilde{K})]^3}^2 + h \sum_{l \subset \partial K} \|\bar{\mathbf{R}} - \mathbf{R}\|_{[L_2(l)]^3}^2 \\ &\quad + (1+k^2)^2\|e_h\|_{\text{curl},\tilde{K}}^2. \end{aligned}$$

Summarizing, we obtained that the error indicator  $\eta_K$  provides a lower bound for the exact error on the patch  $\tilde{K}$  plus some computable remainders (arising from interpolation errors):

$$(56) \quad \eta_K^2 \leq C((1+k^2)^2\|e_h\|_{\text{curl},\tilde{K}}^2 + h^2\|\bar{\mathbf{r}} - \mathbf{r}\|_{[L_2(\tilde{K})]^3}^2 + h\|\bar{\mathbf{R}} - \mathbf{R}\|_{[L_2(\partial K)]^3}^2).$$

Using in addition Lemma 11 we state the main result of this section:

**Theorem 3.** *The implicit a posteriori error estimate  $\hat{e}_h$  can be used as a lower bound for the exact error with respect to the curl norm as follows:*

$$(57) \quad \begin{aligned} \|\hat{e}_h\|_{\text{curl},K} &\leq C_1\eta_K \leq C((1+k^2)^2\|e_h\|_{\text{curl},\tilde{K}}^2 \\ &\quad + h^2\|\bar{\mathbf{r}} - \mathbf{r}\|_{[L_2(\tilde{K})]^3}^2 + h\|\bar{\mathbf{R}} - \mathbf{R}\|_{[L_2(\partial K)]^3}^2)^{1/2}. \end{aligned}$$

*Proof.* We get the desired result immediately using the estimates (42) and (56).  $\square$

*Remarks.* 1. Up to the estimate (56) we kept track of the  $k$ -dependence in the estimates.

2. If the local divergence free property of the estimate  $\hat{e}_h$  is desirable (for example, to ensure the equivalence of some norms in the error estimates [14]), one should enforce this condition by projecting to a divergence free basis. Although the finite element space that we used (see Section 2.1) consists of second order elements as well, the choice of  $V_h$  should be done according to the above requirement, when  $\mathbf{E}_h$  is obtained using a higher order Nédélec space.

3. Another special situation occurs; if  $\text{curl } \mathbf{E}_h = 0$ , then  $\mathbf{R}_{l_j} = 0$ . In this way, one expects that the result in Theorem 3 cannot be sharpened in the sense that neither  $\hat{e}_h$  nor  $\eta_K$  will provide an upper bound for the error. In this case the Helmholtz decomposition (see Lemma 4.5 in [21]) of  $\mathbf{E}_h$  consists of only a gradient which can be non-smooth. For the smoothness of the components in the Helmholtz decomposition we refer to [2], Remark 2.16 and Theorem 2.17. This is in good agreement with the fact that in the proof of upper bounds in residual based error estimation techniques one needs the regularity of solutions ([1, Section 2.2 and



Section 3.2.3]). This can fail for the present solution  $\mathbf{E}$ ; see the test case in Section 5.1.2.

4. The remaining terms in Theorem 3 can make the estimate unsharp when  $\|\bar{\mathbf{r}} - \mathbf{r}\|_{[L_2(K)]^3}$  and  $\|\bar{\mathbf{R}} - \mathbf{R}\|_{[L_2(\partial K)]^3}$  are of the same order as the residuals  $\|\mathbf{r}\|_{[L_2(K)]^3}$  and  $\|\mathbf{R}\|_{[L_2(\partial K)]^3}$ , respectively. This can happen if the right hand side  $\mathbf{J}_k$  is non-smooth or if we take a more general type of Maxwell equation with discontinuous material coefficients. Then in an adaptive refinement technique we should generate  $\mathcal{T}_h$  in such a way that the solution in the subdomains is smooth. If this is not possible (e.g. if we want to avoid the use of curvilinear hexahedra), then some extra refinement should be performed in this critical region.

### 5. NUMERICAL RESULTS

In this section, we demonstrate the performance of the implicit error estimator (11) applied to the time harmonic Maxwell equations. We consider the Maxwell equations on a domain  $\Omega$  which is taken to be a cubic domain or a so-called Fichera cube; see Figure 9.

In order to be able to evaluate the discretization errors, we pick up a vector field  $\mathbf{E}$ , substitute it into the Maxwell equations and choose the source term  $\mathbf{J}_k$  such that  $\mathbf{E}$  is the solution.

Recall that  $\mathbf{E}_h$  denotes the numerical solution of the Maxwell equations (1) obtained by using the edge finite elements given in Section 2.1. In the rest of this section the elements of the tessellation  $\mathcal{T}_h$  are cubes with size  $h \times h \times h$ .

**5.1. Test cases.** We verify the performance of the implicit error estimator for the Maxwell equations on three different test cases. The local problems (11) are solved by using the numerical model discussed in Section 3.2.

Several aspects determine the usefulness of an a posteriori error estimator:

- The error estimator has to be able to find those areas in the domain where the finite element solution has a large error, since this information is for local mesh adaptation.
- The error estimator should be close in magnitude to the real error, both locally and globally.

We check the performance of the implicit error estimator in the following way. First, we check if the estimator provides the right type of error distribution in the domain. Second, the magnitude of the global error estimate and its convergence under mesh refinement are compared with the exact error.

Define the exact error  $\delta_K$  and the implicit *local error estimate*  $\hat{\delta}_K$  on element  $K$  as

$$(58) \quad \delta_K = \|\mathbf{E} - \mathbf{E}_h\|_{\text{curl},K}, \quad \hat{\delta}_K = \|\hat{\mathbf{e}}_h\|_{\text{curl},K}.$$

The exact global error  $\delta$  and the implicit global error estimate  $\delta_h$  are obtained by summing up the local contributions

$$(59) \quad \delta = \left( \sum_{K \in \mathcal{T}_h} \delta_K^2 \right)^{1/2}, \quad \delta_h = \left( \sum_{K \in \mathcal{T}_h} \hat{\delta}_K^2 \right)^{1/2}.$$

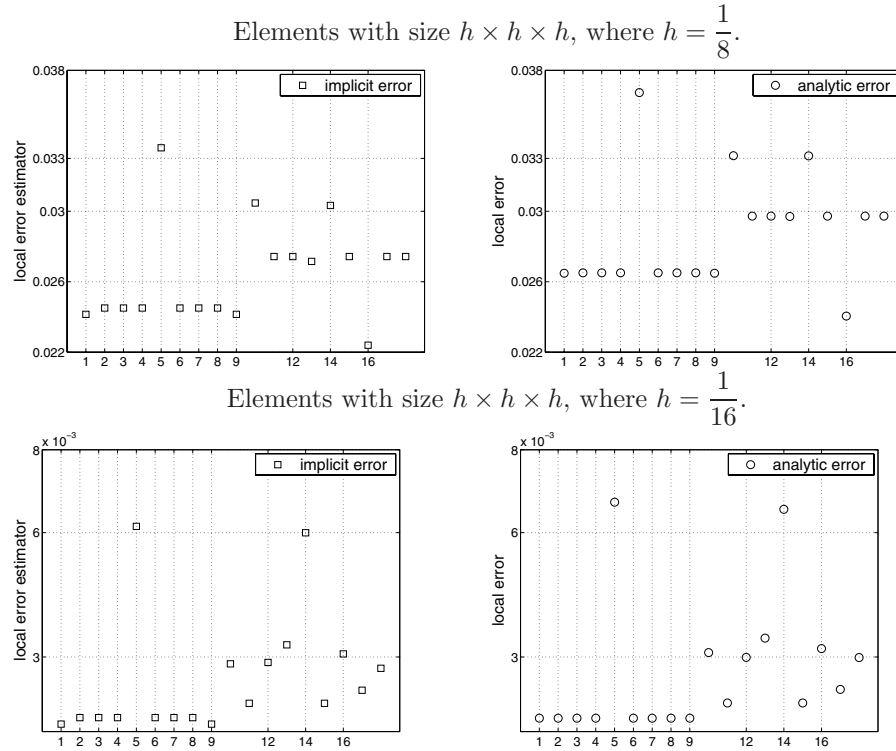


FIGURE 1. Error distribution in the  $H(\text{curl})$  norm for the smooth test case with  $p = m = 1$ .

5.1.1. *Smooth solution.* The first test case we consider are the Maxwell equations (1) on the domain  $\Omega = (0, 1)^3$  with the given source term  $\mathbf{J}_k$  defined as

$$(60) \quad \mathbf{J}_k(x, y, z) = (\pi^2(p^2 + m^2) - 1) \begin{pmatrix} \sin(\pi p y) \sin(\pi m z) \\ \sin(\pi p z) \sin(\pi m x) \\ \sin(\pi p x) \sin(\pi m y) \end{pmatrix},$$

and which have a smooth exact solution

$$(61) \quad \mathbf{E}(x, y, z) = \begin{pmatrix} \sin(\pi p y) \sin(\pi m z) \\ \sin(\pi p z) \sin(\pi m x) \\ \sin(\pi p x) \sin(\pi m y) \end{pmatrix}$$

with  $p, m \in \mathbb{N}$ .

In Figures 1 and 2 we plot the local errors (58) obtained with the implicit error estimator and the exact error on a representative set of elements. The error distribution diagram for the case  $p = 1, m = 1$  is given in Figure 1, and for the case  $p = 5, m = 1$  the results are shown in Figure 2. The locations of some elements where the error is computed in the mesh with mesh size  $h = \frac{1}{16}$  are shown in Figure 3. The labels on the horizontal axis in Figures 1 and 2 refer to the element numbers shown in Figure 3.

The error distribution obtained with the implicit error estimator shows a good agreement with the exact results. In the case  $p = m = 1$ , where the analytic solution

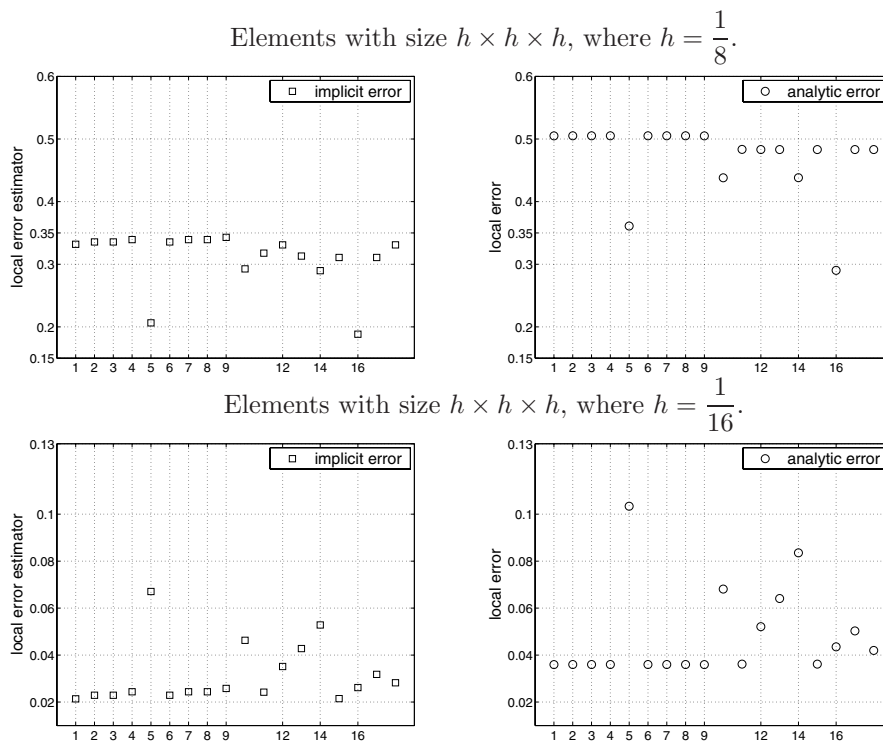


FIGURE 2. Error distribution in the  $H(\text{curl})$  norm for the smooth test case with  $p = 5, m = 1$ .

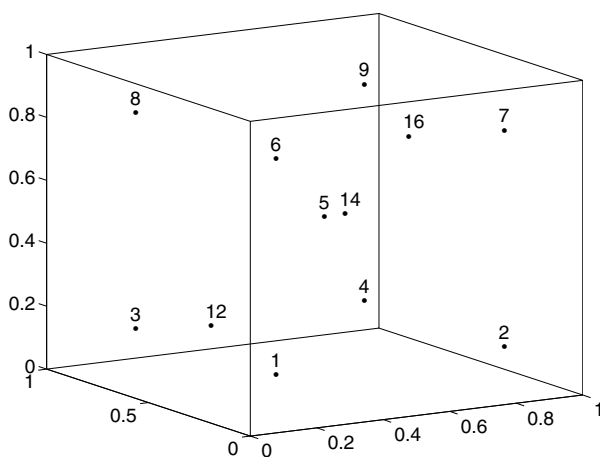


FIGURE 3. Location of some of the elements where the implicit error estimation was conducted (smooth test case) on a mesh with  $h = \frac{1}{16}$ .

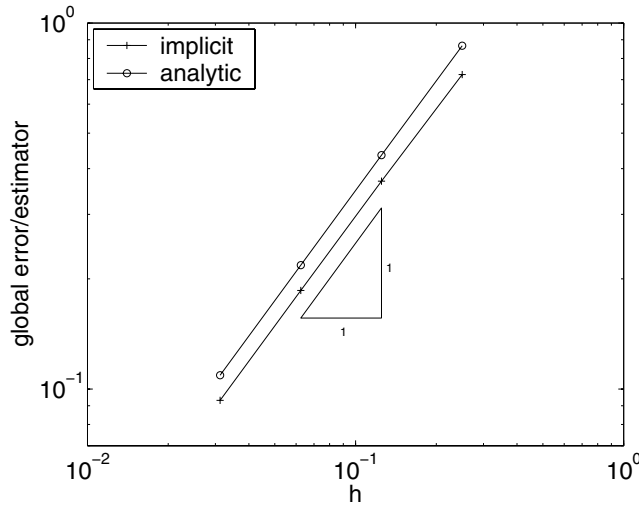


FIGURE 4. The global error estimate and the exact global error in the  $H(\text{curl})$  norm versus the mesh size  $h$  for the smooth test case with  $p = m = 1$ .

has only one period in the domain, the error distribution is very close to the exact one. For the case  $p = 5, m = 1$ , where the analytic solution is more oscillatory, we observe that in some elements the distribution is slightly different, but the scheme is still able to detect subdomains with relatively large errors.

The rate of convergence and a global estimate of the error (59) for the case  $p = m = 1$  are given in Figure 4. It shows the same convergence behavior under mesh refinement as the analytic error. Also, the predicted error magnitude is close to the true error.

5.1.2. *Test case with singularities in the solution.* Let us consider the domain  $\Omega = (-1, 1)^3$  and the function

$$f : \Omega \rightarrow \mathbb{R} \text{ with } f = \max\{|x|, |y|, |z|\}.$$

Define  $\mathbf{E} : \Omega \rightarrow \mathbb{R}^3$  as  $\mathbf{E} := -\nabla f(x, y, z)$ . Then  $\mathbf{E}$  solves the following Maxwell problem:

$$(62) \quad \begin{aligned} \text{curl curl } \mathbf{E} - \mathbf{E} &= \nabla f && \text{in } \Omega, \\ \mathbf{E} \times \boldsymbol{\nu} &= 0 && \text{on } \partial\Omega. \end{aligned}$$

In this example the right hand side function is in  $[L_2(\Omega)]^3$  but the exact solution is not smooth; it is not even in  $[H^{\frac{1}{2}}(\Omega)]^3$ . Therefore, theoretically we cannot guarantee even  $1/2$  order of convergence for the finite element solution. Numerically we have observed almost  $1/2$  order convergence in the  $H(\text{curl})$  norm; see Figure 7. For a similar example we refer to [6], where  $\nabla f$  was smooth and the bilinear form  $B_K$  remained coercive. However, compared to the results given in [6], we could improve the accuracy of the estimator using the implicit error estimation technique (see also Section 5.2).

The error distribution computed on different elements for different values of the mesh size is depicted in Figure 5 and the plot of the global error estimator is given

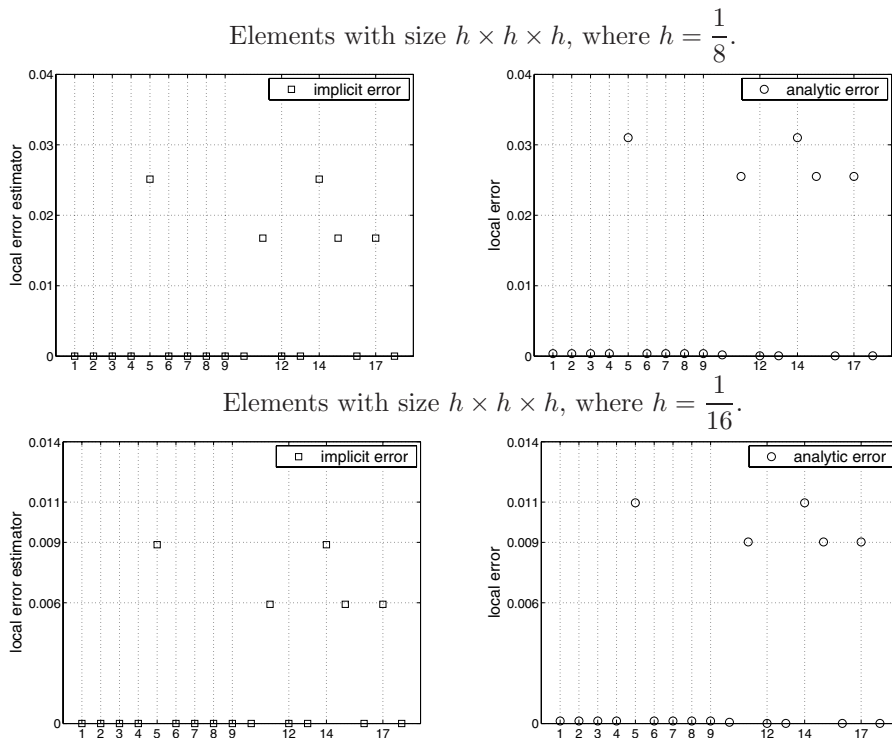


FIGURE 5. Error distribution in the  $H(\text{curl})$  norm for the singular test case.

in Figure 7. The location of the elements on a mesh with  $h = \frac{1}{8}$  is depicted in Figure 6. The labels on the horizontal axis in Figure 5 refer to the elements shown in Figure 6. We observe that the implicit error estimator provides the same type of error distribution as the exact error and also that the estimates are close to the exact values. The convergence rate of the implicit error estimator is of the same order as the exact error.

5.1.3. *Fichera cube.* In this subsection we analyze the method on the Fichera cube  $\Omega = (-1, 1)^3 \setminus [-1, 0]^3$ . The solution on this domain has corner and edge singularities and can serve as a difficult test case. The boundary conditions and the source term in (1) are chosen such that the exact solution is  $\mathbf{E} = \text{grad}(r^{2/3} \sin(\frac{2}{3}\phi))$  in spherical coordinates, with  $r = \sqrt{x^2 + y^2 + z^2}$ ,  $\phi = \arccos \frac{r}{z}$ . It is clear that  $\mathbf{E}$  does not belong to  $[H^1(\Omega)]^3$ .

The error distribution diagram is given in Figure 8. The large errors correspond to those elements which are close to the Fichera corner, located in the point  $(0, 0, 0)$ ; see Figure 9. The plot of the global error estimate is given in Figure 10. As in the previous test cases, we observe a good agreement between the implicit error estimator and the exact errors, both in the error distribution and in the numerical values. The implicit error estimation is clearly capable of providing a rather accurate error estimate for a range of smooth and non-smooth flows, but even more important for an adaptation algorithm, it gives a clear indication of those regions where the

error is large. The numerical results also show that the implicit error estimates are always bounded by the true error, which was proven in Theorem 3.

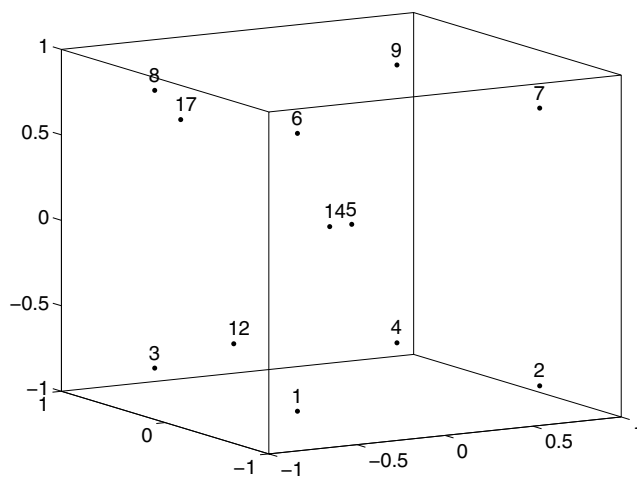


FIGURE 6. Location of some of the elements where the implicit error estimation was conducted (singular test case, Section 5.1.2) on a mesh with  $h = \frac{1}{8}$ .

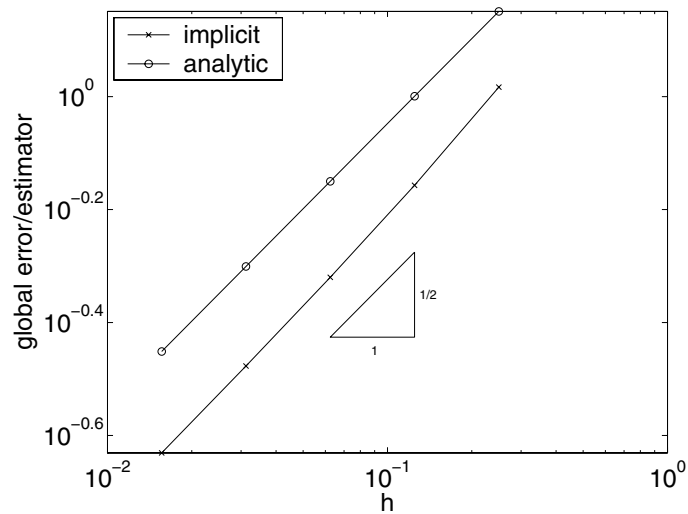


FIGURE 7. The global error estimate and the exact global error in the  $H(\text{curl})$  norm for the singular test case (Section 5.1.2).

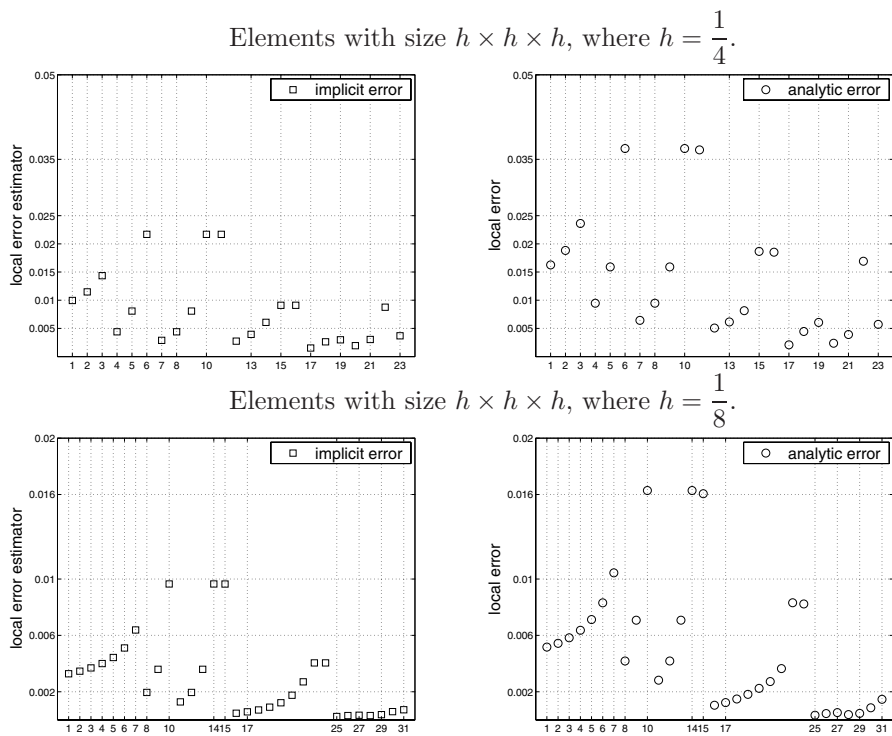


FIGURE 8. Error distribution in the  $H(\text{curl})$  norm on the Fichera cube.

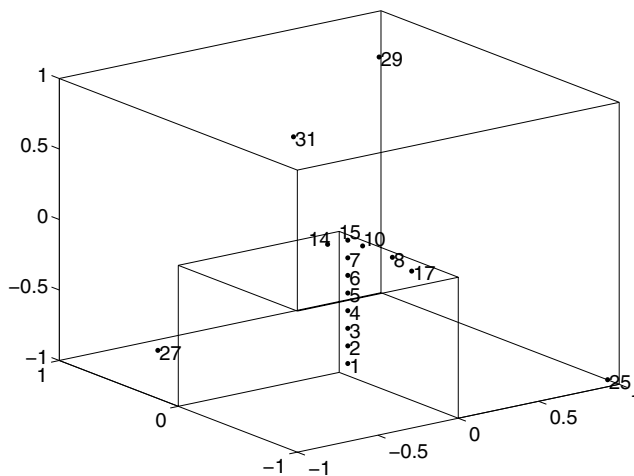


FIGURE 9. Location of some of the elements on the Fichera cube where the implicit error estimation was conducted on a mesh with  $h = \frac{1}{8}$ .

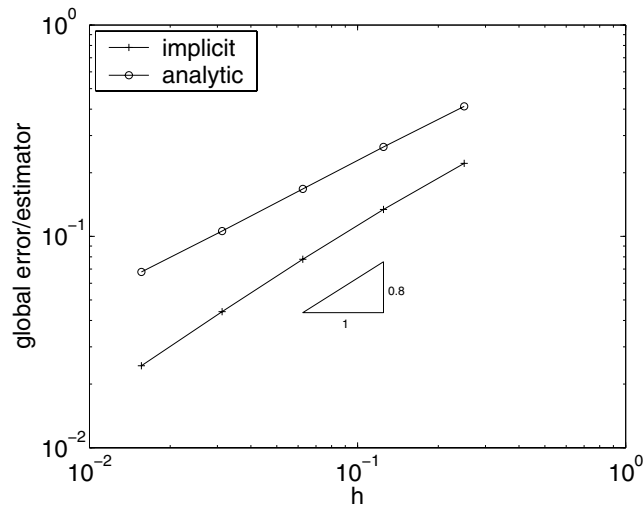


FIGURE 10. The global error estimate and the exact global error in the  $H(\text{curl})$  norm on the Fichera cube.

5.2. **Comparisons with some existing schemes.** In [6] Beck, Hiptmair et al. consider the following elliptic boundary value problem:

$$(63) \quad \begin{aligned} \text{curl}(\chi \text{curl} \mathbf{E}) + \beta \mathbf{E} &= \mathbf{J}_k \quad \text{in } \Omega, \\ \mathbf{E} \times \boldsymbol{\nu} &= 0 \quad \text{on } \partial\Omega, \end{aligned}$$

where  $\chi$  and  $\beta$  are given positive functions on  $\Omega$ .

We apply our implicit error estimator to (63) and compare the results with those given in [6] and [7].

For comparison purposes we consider the first example given in [6] and [7] on the domain  $\Omega = (0, 1)^3$ .

In this example the parameter  $\chi$  is set to one and different values of  $\beta$  are taken into account. The exact solution is rather smooth and is given by  $\mathbf{E} = (0, 0, \sin(\pi x))$ . Roughly speaking, the system (63) reduces to (1) if we choose  $\beta = -k^2$  and no other changes are necessary to the algorithm discussed for (1). Note that the bilinear form for this problem is coercive, contrary to the bilinear form (5) discussed in this paper which is indefinite.

For the finite element solution in the first example in [6] the authors start with a coarse grid (level 0) consisting of 6 tetrahedrons, which is refined uniformly up to five levels. In [6] an adaptive strategy has also been presented for other test cases; see Experiments 6-8 therein. In [7] a hierarchical type (implicit) error estimator is applied using preconditioning for solving the global problems for the error.

We make comparisons in terms of the effectivity index  $\varepsilon_h := \frac{\delta_h}{\delta}$ , which gives the ratio between the estimated and the true global error, where  $\delta$  and  $\delta_h$  are given by (59). This quantity merely reflects the quality of the global estimate, while we are mainly interested in local error estimates. The comparison table of the effectivity of the estimators given in [6], [7] and the implicit error estimator developed in this paper are listed in Table 1. In comparison to the results given in [6] and [7]



TABLE 1. Comparison of the effectivity indices.

$\beta \backslash$ Level	0	1	2	3	4	5
$10^{-4}$	4.05	8.05	8.18	8.24	8.27	8.29
$10^{-2}$	4.05	8.05	8.17	8.23	8.27	8.29
1	3.01	7.64	7.78	7.84	7.87	7.89
$10^2$	2.29	4.27	4.70	4.95	5.20	5.26
$10^4$	2.33	4.23	4.66	4.86	4.95	5.00

Effectivity index  $\varepsilon_h$  for the error estimator given in [6].

$\beta \backslash$ Level	0	1	2	3	4	5
$10^{-4}$	0.55	0.82	0.92	0.96	0.98	0.99
$10^{-2}$	0.55	0.82	0.92	0.96	0.98	0.99
1	0.56	0.83	0.92	0.95	0.97	0.98
$10^2$	0.71	0.87	0.92	0.91	0.90	0.90
$10^4$	0.72	0.88	0.93	0.94	0.94	0.93

Effectivity index  $\varepsilon_h$  for the Gauss-Seidel-based hierarchical error estimator given in [7].

$\beta \backslash h$	$\frac{1}{4}$	$\frac{1}{8}$	$\frac{1}{16}$	$\frac{1}{32}$	$\frac{1}{64}$
$10^{-4}$	0.67	0.67	0.67	0.67	0.67
$10^{-2}$	0.67	0.67	0.67	0.67	0.67
1	0.67	0.67	0.67	0.67	0.67
$10^2$	0.63	0.65	0.67	0.67	0.67
$10^4$	0.44	0.37	0.40	0.53	0.63

Effectivity index  $\varepsilon_h$  for the implicit error estimator given by (11).

the estimates obtained with the implicit error estimator given by (11) are nearly insensitive to the value of  $\beta$ .

The above index is not capable of indicating the correlation between the distribution of the estimated and the exact error, which influences the effectivity of an adaptive technique. Therefore, we investigate a second quantity used for the comparison, the so-called “fraction of incorrect decisions”, denoted by  $\mu^{(1)}$ . This measures how much the refinement controlled by the estimator differs from the refinement based upon an “ideal” estimator. The indicator  $\mu^{(1)}$  is defined using the following sets:

The set of elements marked for refinement by the error estimator are defined as

$$\hat{A} := \left\{ K \in \mathcal{T}_h : \delta_K^2 > \sigma \frac{\delta_h^2}{n_K} \right\},$$

where  $\sigma = 0.95$  and  $n_K$  denotes the number of elements in the tessellation  $\mathcal{T}_h$ , and where the set of elements that should have been marked

$$A := \left\{ K \in \mathcal{T}_h : \delta_K^2 > \sigma \frac{\delta^2}{n_K} \right\}.$$

TABLE 2. Comparison of the “incorrect decisions”.

$\beta \backslash$ Level	0	1	2	3	4	5
$10^{-4}$	0.33	0.17	0.12	0.1	0.1	0.085
$10^{-2}$	0.33	0.17	0.12	0.1	0.1	0.086
1	0.33	0.25	0.18	0.14	0.13	0.13
$10^2$	0	0.42	0.088	0.14	0.15	0.16
$10^4$	0	0.44	0.11	0.15	0.16	0.16

Fraction of incorrect decisions  $\mu^{(1)}$  for the error estimator given in [6].

$\beta \backslash h$	$\frac{1}{4}$	$\frac{1}{8}$	$\frac{1}{16}$	$\frac{1}{32}$	$\frac{1}{64}$
$10^{-4}$	0	0	0	0	0
$10^{-2}$	0	0	0	0	0
1	0	0	0	0	0
$10^2$	0	0	0	0	0
$10^4$	0.25	0.31	0.07	0.00	0.03

Fraction of incorrect decisions  $\mu^{(1)}$  for the implicit error estimator given by (11).

Then the indicator  $\mu^{(1)}$  is defined as

$$(64) \quad \mu^{(1)} := \frac{1}{n_K} \# \left\{ (A \cap \hat{A}^c) \cup (A^c \cap \hat{A}) \right\},$$

where for any set  $S \subset \mathcal{T}_h$  the compliment with respect to  $\mathcal{T}_h$  is denoted by  $S^c$ .

In [6] satisfactory performance of the estimator means that  $\mu^{(1)}$  stays bounded below 1 as refinement proceeds. The results are given in Table 2. For the implicit estimator this parameter is close to 0, which shows a much better performance than that given in [6]. In other words it means that the implicit error estimator developed in this paper is able to find almost all elements which need refinement. The error indicator from [6] gives between 8.5% and 16% error ( $\mu^{(1)} \cdot 100\%$ ) on the finest mesh; see Table 2.

### 6. CONCLUSIONS AND FURTHER WORKS

In this paper we have developed and analyzed an implicit a posteriori error estimation technique for the time harmonic Maxwell equations. The algorithm is well suited both for cases where the bilinear form is coercive and for the more complicated indefinite case. A nice feature of the implicit error estimator is that no unknown constants appear. The algorithm is tested on a number of increasingly complicated test cases and the results show that it gives an accurate prediction of the error distribution and the local and global error. Also, in comparison with other a posteriori error estimation techniques [6, 23], for all considered tests it gives a sharper estimate of the error and its distribution.

In future work we will apply the implicit a posteriori error estimator in an adaptive algorithm and also consider different types of elements including the effect of mesh deformation on hexahedral elements.

APPENDIX A.

For the proof of Lemma 8 we recall some notations and results from linear algebra.

If the symmetric matrix  $A$  is positive semidefinite, we shortly write it as  $A \geq 0$ , while  $A > 0$  is used for positive definite symmetric matrices. We use the fact that the maximal eigenvalue  $\lambda_{A,\max}$  of a symmetric matrix  $A \in \mathbb{R}^{n \times n}$  can be characterized as

$$(65) \quad \lambda_{A,\max} = \max_{\substack{\mathbf{u} \in \mathbb{R}^n \\ |\mathbf{u}|=1}} (A\mathbf{u}, \mathbf{u})$$

and similarly, for the minimal eigenvalue  $\lambda_{A,\min}$  of  $A$

$$(66) \quad \lambda_{A,\min} = \min_{\substack{\mathbf{u} \in \mathbb{R}^n \\ |\mathbf{u}|=1}} (A\mathbf{u}, \mathbf{u}),$$

where  $(\cdot, \cdot)$  yields the standard scalar product in  $\mathbb{R}^n$ . We will also use the notation  $\lambda_{A,\min}^+ > 0$  for the minimal non-zero eigenvalue of a positive semidefinite matrix  $A$ .

For the proof of Lemma 8 we need the following linear algebraic estimate.

**Lemma 12.** *Assume that  $k \in \mathbb{R}$  and the symmetric matrices  $A \geq 0, B > 0$  in  $\mathbb{R}^{n \times n}$  are given such that  $\ker A$  is an invariant space of  $B$ . Then, there are constants  $c, h_0 \in \mathbb{R}^+$  such that for any  $h$  with  $0 < h < h_0$  and any  $\mathbf{u} \in \mathbb{R}^n$  there is a  $\mathbf{v} \in \mathbb{R}^n$  such that*

$$(67) \quad |((\frac{1}{h^2}A - k^2B)\mathbf{u}, \mathbf{v})|^2 \geq c((\frac{1}{h^2}A + B)\mathbf{u}, \mathbf{u})((\frac{1}{h^2}A + B)\mathbf{v}, \mathbf{v}).$$

*Proof.* In the proof we assume that  $k \geq 1$ . The remaining case can be handled in the same way; we have only to consider  $k^2B$  instead of  $B$ .

According to the assumptions every  $\mathbf{u} \in \mathbb{R}^n$  can be decomposed as  $\mathbf{u} = \mathbf{u}_1 + \mathbf{u}_2$ , where  $\mathbf{u}_1 \in \ker A$  and  $\mathbf{u}_2 \perp \ker A$ . Note that according to the assumptions,  $B\mathbf{u}_1 \in \ker A$  and therefore,  $(B\mathbf{u}_1, \mathbf{v}_2) = 0$  for all  $\mathbf{v}_2 \perp \ker A$ .

We distinguish two cases:

*Case 1.*  $\mathbf{u}_1 = 0$ . Then we can choose  $\mathbf{v} = \mathbf{u} = \mathbf{u}_2$  and  $h_0$  such that

$$(68) \quad k^2\lambda_{B,\max} \leq \frac{1}{2h_0^2}\lambda_{A,\min}^+.$$

In this way, the characterizations in (65) and (66) imply that for any  $0 < h < h_0$  the eigenvalues of the matrix  $\frac{1}{h^2}A - k^2B$  will be positive and their minimum is at least  $\frac{1}{2h_0}\lambda_{A,\min}^+$ . With these the left hand side of (67) can be estimated as

$$|((\frac{1}{h^2}A - k^2B)\mathbf{u}_2, \mathbf{u}_2)|^2 \geq (\frac{1}{2h_0}\lambda_{A,\min}^+|\mathbf{u}_2|^2)^2.$$

The scalar products on the right hand side of (67) can also be estimated (using (68)) as follows:

$$\begin{aligned} ((\frac{1}{h^2}A + B)\mathbf{u}, \mathbf{u})((\frac{1}{h^2}A + B)\mathbf{v}, \mathbf{v}) &= ((\frac{1}{h^2}A + B)\mathbf{u}_2, \mathbf{u}_2)((\frac{1}{h^2}A + B)\mathbf{u}_2, \mathbf{u}_2) \\ &\leq (\frac{2}{h_0^2}\lambda_{A,\max}|\mathbf{u}_2|^2)^2. \end{aligned}$$

Therefore, the choice  $c = \left(\frac{1}{4} \frac{\lambda_{A,\min}^+}{\lambda_{A,\max}}\right)^2$  is appropriate in the first case.

*Case 2.*  $\mathbf{u}_1 \neq 0$ . We now choose  $\mathbf{v} = \mathbf{u}_1 - \mathbf{u}_2$ . The left hand side of (67) can be then rewritten as

$$\begin{aligned}
 & |((\frac{1}{h^2}A - k^2B)\mathbf{u}, \mathbf{v})|^2 \\
 &= |((\frac{1}{h^2}A - k^2B)(\mathbf{u}_1 + \mathbf{u}_2), \mathbf{u}_1 - \mathbf{u}_2)|^2 \\
 (69) \quad &= |((\frac{1}{h^2}A - k^2B)\mathbf{u}_1, \mathbf{u}_1) - ((\frac{1}{h^2}A - k^2B)\mathbf{u}_2, \mathbf{u}_2)|^2 \\
 &= | -k^2(B\mathbf{u}_1, \mathbf{u}_1) - ((\frac{1}{h^2}A - k^2B)\mathbf{u}_2, \mathbf{u}_2)|^2 \\
 &= k^4|(B\mathbf{u}_1, \mathbf{u}_1)|^2 + 2k^2(B\mathbf{u}_1, \mathbf{u}_1)((\frac{1}{h^2}A - k^2B)\mathbf{u}_2, \mathbf{u}_2) \\
 &\quad + |((\frac{1}{h^2}A - k^2B)\mathbf{u}_2, \mathbf{u}_2)|^2.
 \end{aligned}$$

The right hand side of (67) can be simplified according to the following equality:

$$\begin{aligned}
 & ((\frac{1}{h^2}A + B)\mathbf{u}, \mathbf{u})((\frac{1}{h^2}A + B)\mathbf{v}, \mathbf{v}) \\
 (70) \quad &= ((\frac{1}{h^2}A + B)(\mathbf{u}_1 + \mathbf{u}_2), \mathbf{u}_1 + \mathbf{u}_2)((\frac{1}{h^2}A + B)(\mathbf{u}_1 - \mathbf{u}_2), \mathbf{u}_1 - \mathbf{u}_2) \\
 &= ((B\mathbf{u}_1, \mathbf{u}_1) + ((\frac{1}{h^2}A + B)\mathbf{u}_2, \mathbf{u}_2))^2 \\
 &= |(B\mathbf{u}_1, \mathbf{u}_1)|^2 + 2(B\mathbf{u}_1, \mathbf{u}_1)((\frac{1}{h^2}A + B)\mathbf{u}_2, \mathbf{u}_2) + |((\frac{1}{h^2}A + B)\mathbf{u}_2, \mathbf{u}_2)|^2.
 \end{aligned}$$

Comparing (69) and (70), using the fact that  $k \geq 1$ , the positive definiteness of  $B$  and choosing  $c = \frac{1}{2}$ , then a sufficient condition for the inequality to hold is that we need an  $h_0$  such that for any  $h$  with  $0 < h < h_0$  and for all  $\mathbb{R}^n \ni \mathbf{u}_2 \perp \ker A$  the following inequality holds:

$$((\frac{1}{h^2}A - k^2B)\mathbf{u}_2, \mathbf{u}_2) \geq \frac{1}{2}((\frac{1}{h^2}A + B)\mathbf{u}_2, \mathbf{u}_2).$$

In fact we need that the matrix  $\frac{1}{2h^2}A - (k^2 + \frac{1}{2})B$  is positive semidefinite. According to *Case 1* this holds whenever  $h_0$  is chosen according to the inequality

$$(71) \quad (k^2 + \frac{1}{2})\lambda_{B, \max} \leq \frac{1}{2h_0^2}\lambda_{A, \min}^+.$$

Comparing the estimates in (68) and (71) gives that the choice

$$(72) \quad h_0^2 \leq \frac{1}{2k^2 + 1} \frac{\lambda_{A, \min}^+}{\lambda_{B, \max}}$$

is sufficient in both cases. □

Using this result we can prove Lemma 8.

*Proof of Lemma 8.* Using the notations introduced in Section 4.2 and a simple change of variables we obtain that the mass matrix on a cube  $K$  with edge length  $h$  can be written as

$$B_{1,K} = \frac{1}{h}B_{1, \text{curl}} - k^2hB_{1,0}$$

and accordingly, for  $\mathbf{u} = \sum_{i=1}^n u_i \phi_i \in V_h$  and  $\mathbf{v} = \sum_{i=1}^n v_i \phi_i \in V_h$

$$(73) \quad B_K(\mathbf{u}, \mathbf{v}) = \left( \left( \frac{1}{h} B_{1,\text{curl}} - k^2 h B_{1,0} \right) (u_1, u_2, \dots, u_n)^T, (v_1, v_2, \dots, v_n)^T \right).$$

In the same way,

$$(74) \quad \|\mathbf{u}\|_{\text{curl},K}^2 = \left( \left( \frac{1}{h} B_{1,\text{curl}} + h B_{1,0} \right) (u_1, u_2, \dots, u_n)^T, (u_1, u_2, \dots, u_n)^T \right).$$

Substituting (73) and (74) into the desired inequality (40) we have to find positive constants  $h_0$  and a  $C_0 > 0$  such that for any  $0 < h < h_0$  and any  $\mathbf{u} \in \mathbb{R}^n$  there is a  $\mathbf{v} \in \mathbb{R}^n$  such that

$$(75) \quad C_0 \left( \left( \frac{1}{h} B_{1,\text{curl}} - k^2 h B_{1,0} \right) \mathbf{u}, \mathbf{v} \right)^2 \geq \left( \left( \frac{1}{h} B_{1,\text{curl}} + h B_{1,0} \right) \mathbf{u}, \mathbf{u} \right) \left( \left( \frac{1}{h} B_{1,\text{curl}} + h B_{1,0} \right) \mathbf{v}, \mathbf{v} \right).$$

Dividing both sides with  $h^2$ , we can apply Lemma 12 with  $A = B_{1,\text{curl}}$  and  $B = B_{1,0}$ . For this, we have to check that the conditions in Lemma 12 hold.

A lengthy computation gives that

$$B_{1,\text{curl}} = \frac{1}{1080} \begin{pmatrix} 8 & 4 & -1 & 1 & -1 & 1 & 2 & 0 & 0 \\ 4 & 8 & 1 & -1 & 1 & -1 & 2 & 0 & 0 \\ -1 & 1 & 8 & 4 & -1 & 1 & 0 & 2 & 0 \\ 1 & -1 & 4 & 8 & 1 & -1 & 0 & 2 & 0 \\ -1 & 1 & -1 & 1 & 8 & 4 & 0 & 0 & 2 \\ 1 & -1 & 1 & -1 & 4 & 8 & 0 & 0 & 2 \\ 2 & 2 & 0 & 0 & 0 & 0 & 4/5 & 0 & 0 \\ 0 & 0 & 2 & 2 & 0 & 0 & 0 & 4/5 & 0 \\ 0 & 0 & 0 & 0 & 2 & 2 & 0 & 0 & 4/5 \end{pmatrix}$$

and

$$B_{1,0} = \frac{1}{1080} \begin{pmatrix} 2/5 & 1/5 & 0 & 0 & 0 & 0 & 1/10 & 0 & 0 \\ 1/5 & 2/5 & 0 & 0 & 0 & 0 & 1/10 & 0 & 0 \\ 0 & 0 & 2/5 & 1/5 & 0 & 0 & 0 & 1/10 & 0 \\ 0 & 0 & 1/5 & 2/5 & 0 & 0 & 0 & 1/10 & 0 \\ 0 & 0 & 0 & 0 & 2/5 & 1/5 & 0 & 0 & 1/10 \\ 0 & 0 & 0 & 0 & 1/5 & 2/5 & 0 & 0 & 1/10 \\ 1/10 & 1/10 & 0 & 0 & 0 & 0 & 1/25 & 0 & 0 \\ 0 & 0 & 1/10 & 1/10 & 0 & 0 & 0 & 1/25 & 0 \\ 0 & 0 & 0 & 0 & 1/10 & 1/10 & 0 & 0 & 1/25 \end{pmatrix}.$$

By definition, for any vector  $\mathbf{u} = (u_1, u_2, \dots, u_n) \in \mathbb{R}^n$

$$(76) \quad (B_{1,\text{curl}} \mathbf{u}, \mathbf{u}) = \left( \text{curl} \sum_{i=1}^9 u_i \phi_i^0, \text{curl} \sum_{i=1}^9 u_i \phi_i^0 \right)_{[L_2(\hat{K})]^3} = \left\| \text{curl} \sum_{i=1}^9 u_i \phi_i^0 \right\|_{[L_2(\hat{K})]^3}^2,$$

where the basis  $\{\phi_i^0\}_{i=1}^9$  is defined in (3.2.2). Similarly,

$$(B_{1,0} \mathbf{u}, \mathbf{u}) = \left( \sum_{i=1}^9 u_i \phi_i^0, \sum_{i=1}^9 u_i \phi_i^0 \right)_{[L_2(\hat{K})]^3} = \left\| \sum_{i=1}^9 u_i \phi_i^0 \right\|_{[L_2(\hat{K})]^3}^2,$$

which show that  $B_{1,\text{curl}} \geq 0$  and  $B_{1,0} > 0$ . Moreover (76) gives that for any non-zero vector  $\mathbf{u} \in \mathbb{R}^n$  the condition  $(B_{1,\text{curl}} \mathbf{u}, \mathbf{u}) = 0$  can only be fulfilled if  $\text{curl} \sum_{i=1}^9 u_i \phi_i^0 = \mathbf{0}$ .

In order to determine such a linear combination, observe that an arbitrary element  $\hat{\Phi}$  in the finite dimensional bubble function space  $\hat{V}$  given in (3.2.2) can be written as

$$\hat{\Phi}(\xi, \eta, \zeta) = \begin{pmatrix} (a_1\xi^2 + b_1\xi + c_1)\eta(1-\eta)\zeta(1-\zeta) \\ \xi(1-\xi)(a_2\eta^2 + b_2\eta + c_2)\zeta(1-\zeta) \\ \xi(1-\xi)\eta(1-\eta)(a_3\zeta^2 + b_3\zeta + c_3) \end{pmatrix}$$

and accordingly,

$$\begin{aligned} &\text{curl } \hat{\Phi}(\xi, \eta, \zeta) \\ &= \begin{pmatrix} \xi(1-\xi)(1-2\eta)(a_3\zeta^2 + b_3\zeta + c_3) - \xi(1-\xi)(a_2\eta^2 + b_2\eta + c_2)(1-2\zeta) \\ (a_1\xi^2 + b_1\xi + c_1)\eta(1-\eta)(1-2\zeta) - (1-2\xi)\eta(1-\eta)(a_3\zeta^2 + b_3\zeta + c_3) \\ (1-2\xi)(a_2\eta^2 + b_2\eta + c_2)\zeta(1-\zeta) - (a_1\xi^2 + b_1\xi + c_1)(1-2\eta)\zeta(1-\zeta) \end{pmatrix}. \end{aligned}$$

This can be zero on  $\hat{K}$  if the following equalities hold:

$$\begin{aligned} (1-2\eta)(a_3\zeta^2 + b_3\zeta + c_3) &= (a_2\eta^2 + b_2\eta + c_2)(1-2\zeta), \\ (a_1\xi^2 + b_1\xi + c_1)(1-2\zeta) &= (1-2\xi)(a_3\zeta^2 + b_3\zeta + c_3), \\ (1-2\xi)(a_2\eta^2 + b_2\eta + c_2) &= (a_1\xi^2 + b_1\xi + c_1)(1-2\eta). \end{aligned}$$

Here using the first equation we obtain that

$$a_2 = a_3 = 0, \quad \frac{b_2}{c_2} = \frac{b_3}{c_3} = -2, \quad b_2 = b_3, \quad c_2 = c_3$$

or, alternatively,  $a_2 = a_3 = b_2 = c_2 = b_3 = c_3 = 0$ . Similarly, the second one gives that

$$a_3 = a_1 = 0, \quad \frac{b_3}{c_3} = \frac{b_1}{c_1} = -2, \quad b_3 = b_1, \quad c_3 = c_1$$

or, alternatively,  $a_1 = a_3 = b_3 = c_3 = b_1 = c_1 = 0$ . The third equation is trivially satisfied with these coefficients. We may assume that  $c_1 = 1$  and in this way,  $c_1 = c_2 = c_3 = 1$  and  $b_1 = b_2 = b_3 = -2$ . This gives the eigenfunction

$$(77) \quad (\xi, \eta, \zeta) \rightarrow \begin{pmatrix} (1-2\xi)\eta(1-\eta)\zeta(1-\zeta) \\ \xi(1-\xi)(1-2\eta)\zeta(1-\zeta) \\ \xi(1-\xi)\eta(1-\eta)(1-2\zeta) \end{pmatrix}$$

which is a linear combination  $\sum_{i=1}^9 u_i \Phi_i^0$ , with  $\mathbf{u} = (1, -1, 1, -1, 1, -1, 0, 0, 0)^T$ . This gives that  $\ker B_{1,\text{curl}} = \text{span}(1, -1, 1, -1, 1, -1, 0, 0, 0)$ , which is an invariant space of  $B_{1,0}$  since  $B_{1,0}(\ker B_{1,\text{curl}}) = \ker B_{1,\text{curl}}$ . In this way, the conditions in Lemma 12 are fulfilled for  $A = B_{1,\text{curl}}$  and  $B = B_{1,0}$ , which gives the statement in Lemma 8.  $\square$

*Proof of Lemma 9.* Symbolic calculations give that  $\lambda_{B_{1,\text{curl}},\text{min}}^+ = \frac{4}{675} - \frac{\sqrt{246}}{2700}$  and  $\lambda_{B_{1,0},\text{max}} = \frac{1}{3375} + \frac{\sqrt{246}}{54000}$ .

Using the above numerical results and substituting them into (72) we obtain the statement of Lemma 9.  $\square$

*Remarks.* 1. In the proof of Lemma 8 we determined that the kernel of the curl operator in the bubble function space is the one dimensional subspace generated by the function in (77). This coincides with the subspace of the bubble function space which consists of discrete gradients, namely (77) is the gradient of the function given by

$$(\xi, \eta, \zeta) \rightarrow (\xi(1-\xi), \eta(1-\eta), \zeta(1-\zeta)).$$

2. The reason why we did not include  $k$  into the matrix  $B$  in Lemma 12 is that we wanted to demonstrate the dependence of the mesh size parameter  $h_0$  on  $k$ .

3. An easy calculation gives that for  $K = (0, h)^3$  the condition number of  $B_{1,K}$  is proportional to  $h^{-2}$ . However, this does not harm the solution of the local problem due to Lemma 8.

## ACKNOWLEDGEMENTS

We would like to thank Dr. M. A. Botchev for valuable discussions on the linear algebra problems and useful comments on the text.

## REFERENCES

- [1] M. Ainsworth and J. T. Oden. *A posteriori error estimation in finite element analysis*. Pure and Applied Mathematics. Wiley-Interscience [John Wiley & Sons], New York, 2000. MR1885308 (2003b:65001)
- [2] C. Amrouche, C. Bernardi, M. Dauge, and V. Girault. Vector potentials in three-dimensional non-smooth domains. *Math. Methods Appl. Sci.*, 21(9):823–864, 1998. MR1626990 (99e:35037)
- [3] I. Babuska and T. Strouboulis. *The finite element method and its reliability*. Clarendon Press, Oxford, 2001. MR1857191 (2002k:65001)
- [4] W. Bangerth and R. Rannacher. *Adaptive finite element methods for differential equations*. Lectures in Mathematics. Birkhäuser, Basel, 2003. MR1960405 (2004b:65002)
- [5] R. E. Bank and R. K. Smith. A posteriori error estimates based on hierarchical bases. *SIAM J. Numer. Anal.*, 30(4):921–935, 1993. MR1231320 (95f:65212)
- [6] R. Beck, R. Hiptmair, R. H. W. Hoppe, and B. Wohlmuth. Residual based a posteriori error estimators for eddy current computation. *M2AN Math. Model. Numer. Anal.*, 34(1):159–182, 2000. MR1735971 (2000k:65203)
- [7] R. Beck, R. Hiptmair, and B. Wohlmuth. Hierarchical error estimator for eddy current computation. In *Numerical mathematics and advanced applications (Jyväskylä, 1999)*, pages 110–120. World Sci. Publishing, River Edge, NJ, 2000. MR1936173
- [8] S. C. Brenner and L. R. Scott. *The mathematical theory of finite element methods*, volume 15 of *Texts in Applied Mathematics*. Springer-Verlag, New York, second edition, 2002. MR1894376 (2003a:65103)
- [9] F. Brezzi, L. P. Franca, T. J. R. Hughes, and A. Russo.  $b = \int g$ . *Comput. Methods Appl. Mech. Engrg.*, 145(3-4):329–339, 1997. MR1456019 (98g:65086)
- [10] A. Buffa and P. Ciarlet, Jr. On traces for functional spaces related to Maxwell’s equations. II. Hodge decompositions on the boundary of Lipschitz polyhedra and applications. *Math. Methods Appl. Sci.*, 24(1):31–48, 2001. MR1809492 (2002b:78025)
- [11] A. Buffa, M. Costabel, and D. Sheen. On traces for  $\mathbf{H}(\mathbf{curl}, \Omega)$  in Lipschitz domains. *J. Math. Anal. Appl.*, 276(2):845–867, 2002. MR1944792 (2004i:35045)
- [12] W. Cecot, W. Rachowicz, and L. Demkowicz. An  $hp$ -adaptive finite element method for electromagnetics. III. A three-dimensional infinite element for Maxwell’s equations. *Internat. J. Numer. Methods Engrg.*, 57(7):899–921, 2003. MR1984585 (2004f:78039)
- [13] R. Dautray and J.-L. Lions. *Mathematical analysis and numerical methods for science and technology. Vol. 3*. Springer-Verlag, Berlin, 1990. Spectral theory and applications, With the collaboration of Michel Artola and Michel Cessenat, Translated from the French by John C. Amson. MR1064315 (91h:00004a)
- [14] L. Demkowicz. A posteriori error analysis for steady-state Maxwell’s equations. In *Advances in adaptive computational methods in mechanics (Cachan, 1997)*, volume 47 of *Stud. Appl. Mech.*, pages 513–526. Elsevier, Amsterdam, 1998. MR1644507
- [15] L. Demkowicz. Finite element methods for Maxwell equations. In *Encyclopedia of Computational Mechanics*, pages 723–737. John Wiley & Sons, Chichester, 2004.
- [16] L. Demkowicz and L. Vardapetyan. Modeling of electromagnetic absorption/scattering problems using  $hp$ -adaptive finite elements. *Comput. Methods Appl. Mech. Engrg.*, 152(1-2):103–124, 1998. Symposium on Advances in Computational Mechanics, Vol. 5 (Austin, TX, 1997). MR1602771 (99b:78003)

- [17] A. Ern and J.-L. Guermond. *Theory and practice of finite elements*. Springer-Verlag, New York, 2004. MR2050138 (2005d:65002)
- [18] M. B. Giles and E. Süli. Adjoint methods. *Acta Numerica*, 11:145–236, 2002. MR2009374 (2005d:65190)
- [19] F. Izsák, D. Harutyunyan, and J. J. W. van der Vegt. *Implicit a posteriori error estimates for the Maxwell equations*. Internal report, Dept. of Appl. Math., University of Twente, Netherlands, 2007. <http://eprints.eemcs.utwente.nl/8448/>.
- [20] J. E. Marsden and T. J. R. Hughes. *Mathematical foundations of elasticity*. Dover Publications Inc., New York, 1994. Corrected reprint of the 1983 original. MR1262126 (95h:73022)
- [21] P. Monk. *Finite Element Methods for Maxwell Equations*. Numerical Mathematics and Scientific Computation. Oxford University Press, Oxford, 2003. MR2059447 (2005d:65003)
- [22] J.-C. Nédélec. Mixed finite elements in  $\mathbf{R}^3$ . *Numer. Math.*, 35(3):315–341, 1980. MR592160 (81k:65125)
- [23] S. Nicaise and E. Creusé. A posteriori error estimation for the heterogeneous Maxwell equations on isotropic and anisotropic meshes. *Calcolo*, 40(4):249–271, 2003. MR2025712 (2004j:65133)
- [24] W. Rachowicz and L. Demkowicz. An *hp*-adaptive finite element method for electromagnetics. part I: data structure and constrained approximation. *Comput. Methods Appl. Mech. Engrg.*, 187(1-2):307–337, 2000.
- [25] W. Rachowicz and L. Demkowicz. An *hp*-adaptive finite element method for electromagnetics. II. A 3D implementation. *Internat. J. Numer. Methods Engrg.*, 53(1):147–180, 2002. *p* and *hp* finite element methods: mathematics and engineering practice (St. Louis, MO, 2000). MR1870737 (2002j:78030)
- [26] W. Rachowicz and A. Zdunek. An *hp*-adaptive finite element method for scattering problems in computational electromagnetics. *Internat. J. Numer. Methods Engrg.*, 62(9):1226–1249, 2005. MR2120293 (2005k:78010)
- [27] G. Rodrigue and D. White. A vector finite element time-domain method for solving Maxwell's equations on unstructured hexahedral grids. *SIAM Journal on Scientific Computing*, 23(3):683–706, 2001. MR1860960 (2002h:78036)
- [28] R. Verfürth. *A Review of A Posteriori Error Estimation and Adaptive Mesh-Refinement Techniques*. Advances in Numerical Mathematics. Wiley - Teubner, Chichester - Stuttgart, 1996.
- [29] A. Zdunek and W. Rachowicz. Application of the *hp* adaptive finite element method to the three-dimensional scattering of time-harmonic electromagnetic waves. In *Proceedings of the European Conference on Computational Mechanics (Cracow, Poland, 2001)*, 2001.

DEPARTMENT OF APPLIED MATHEMATICS, UNIVERSITY OF TWENTE, P.O. BOX 217, 7500 AE ENSCHEDE, THE NETHERLANDS

*Current address:* ELTE TTK, Department of Applied Analysis and Computational Mathematics, P.O. Box 120, 1518 Budapest, Hungary

*E-mail address:* [izsakf@cs.elte.hu](mailto:izsakf@cs.elte.hu)

DEPARTMENT OF APPLIED MATHEMATICS, UNIVERSITY OF TWENTE, P.O. BOX 217, 7500 AE ENSCHEDE, THE NETHERLANDS

*Current address:* Department of Mathematics and Computer Science, Technische Universiteit Eindhoven, P.O. Box 513, 5600 MB Eindhoven, The Netherlands

*E-mail address:* [d.harutyunyan@tue.nl](mailto:d.harutyunyan@tue.nl)

DEPARTMENT OF APPLIED MATHEMATICS, UNIVERSITY OF TWENTE, P.O. BOX 217, 7500 AE ENSCHEDE, THE NETHERLANDS

*E-mail address:* [j.j.w.vandervegt@math.utwente.nl](mailto:j.j.w.vandervegt@math.utwente.nl)